Materials Horizons

ROYAL SOCIETY OF CHEMISTRY

REVIEW

View Article Online
View Journal | View Issue

Cite this: *Mater. Horiz.*, 2024, **11**, 5815

Photodynamic therapy with NIR-II probes: review on state-of-the-art tools and strategies

Yiqian Yang,[a] Shaohua Jiang,[b] Stefan G. Stanciu,[c] Hao Peng,*[a] Aiguo Wu*[a] and Fang Yang*[a]

In 2022 10% of the world's population was aged 65+, and by 2100 this segment is expected to hit 25%. These demographic changes place considerable pressure over healthcare systems worldwide, which results in an urgent need for accurate, inexpensive and non-invasive ways to treat cancers, a family of diseases correlated with age. Among the therapeutic tools that gained important attention in this context, photodynamic therapies (PDT), which use photosensitizers to produce cytotoxic substances for selectively destroying tumor cells and tissues under light irradiation, profile as important players for next-generation nanomedicine. However, the development of clinical applications is progressing at slow pace, due to still pending bottlenecks, such as the limited tissue penetration of the excitation light, and insufficient targeting performance of the therapeutic probes to fully avoid damage to normal cells and tissues. The penetration depth of long-wavelength near infrared (NIR) light is significantly higher than that of short-wavelength UV and visible light, and thus NIR light in the second window (NIR-II) is acknowledged as the preferred phototherapeutic means for eliminating deep-seated tumors, given the higher maximum permissible exposure, reduced phototoxicity and low autofluorescence, among others. Upon collective multidisciplinary efforts of experts in materials science, medicine and biology, multifunctional NIR-II inorganic or organic photosensitizers have been widely developed. This review overviews the current state-of-the art on NIR-II-activated photosensitizers and their applications for the treatment of deep tumors. We also place focus on recent efforts that combine NIR-II activated PDT with other complementary therapeutic routes such as photothermal therapy, chemotherapy, immunotherapy, starvation, and gas therapies. Finally, we discuss still pending challenges and problems of PDT and provide a series of perspectives that we find useful for further extending the state-of-the art on NIR-II-triggered PDT.

Received 27th June 2024,
Accepted 12th August 2024

DOI: 10.1039/d4mh00819g

rsc.li/materials-horizons

Wider impact

With the growing demand for accurate and non-invasive cancer treatments, photodynamic therapy (PDT) has gained extensive attention. PDT uses photosensitizers to generate cytotoxic substances that selectively destroy tumor tissues under light irradiation. NIR light in the second window (NIR-II) is recognized as the preferred phototherapeutic method for targeting deep-seated tumors due to its higher maximum permissible exposure, reduced phototoxicity, and low autofluorescence, among other advantages. This review summarizes the current advancements in NIR-II-activated photosensitizers and their applications in treating deep tumors. Additionally, it explores the combination of PDT with other therapies to address the limitations of PDT and enhance its efficiency. We hope this review will deepen the understanding of existing gaps in PDT research and inspire the design of advanced, high-performance photosensitizers.

[a] *Laboratory of Advanced Theranostic Materials and Technology, Ningbo Key Laboratory of Biomedical Imaging Probe Materials and Technology, Zhejiang International Cooperation Base of Biomedical Materials Technology and Application, Ningbo Cixi Institute of Biomedical Engineering, Ningbo Institute of Materials Technology and Engineering, Chinese Academy of Sciences, Ningbo 315201, China. E-mail: penghao@nimte.ac.cn, aiguo@nimte.ac.cn, yangf@nimte.ac.cn*

[b] *Jiangsu Co-Innovation Center of Efficient Processing and Utilization of Forest Resources, International Innovation Center for Forest Chemicals and Materials, College of Materials Science and Engineering, Nanjing Forestry University, Nanjing 210037, China*

[c] *Center for Microscopy-Microanalysis and Information Processing, National University of Science and Technology Politehnica Bucharest, Bucharest 060042, Romania*

1. Introduction

Considering factors such as increased life expectancy, given improved healthcare, declining birth rates, and the post-World War II baby boom, the world's population is aging, a demographic shift that can be observed in many countries across the globe. The incidence of age-related diseases is also rapidly increasing, which places tremendous pressure on the sustainability of healthcare systems worldwide. Associated aspects such as accumulation of genetic changes, reduced DNA repair mechanisms, weakened immune system or environmental exposures over time, make aging to be considered one of the most significant risk factors for cancer. However, while age is a significant factor, cancer can still occur at any age, and currently this family of diseases is considered among the greatest threats to human life,[1,2] with their progression being rapid, and many times silent, undetectable until late, untreatable, stages. According to the latest statistics,[3,4] a total of 19 million new cancer cases and 9 million cancer deaths were estimated worldwide in 2020. When identified early, the chances of curing cancer are considerably higher, but many of the current treatments still have prohibitive costs. Furthermore, traditional clinical therapies for treating cancers, including chemotherapy and radiotherapy, exhibit important drawbacks such as patient exhaustion, poor tumor selectivity, systemic toxicity, impaired liver and kidney function, poor prognosis, among others.[5–7] Therefore, the quest for safe, efficient, patient friendly and affordable diagnostic and therapeutic means has become a research hotspot over the recent years. Among various therapeutic solutions that profile as candidates to lay at the foundation of next-generation cancer treatment frameworks and protocols, in the clinic, photodynamic therapy (PDT) has

Yiqian Yang

Yiqian Yang got a master degree in physical chemistry from Shanghai University in 2024. Now she is a PhD candidate jointly trained at the University of Nottingham Ningbo China (UNNC), and the Ningbo Institute of Materials Technology and Engineering, Chinese Academy of Sciences (NIMTE). Her research focuses on the preparation and biomedical applications of nanomaterials, especially ferrite nanoparticles doping with transition metal ions.

Hao Peng

Hao Peng obtained his PhD degree from the Ningbo Institute of Materials Technology and Engineering, Chinese Academy of Sciences in 2022 and is now carrying out his post-doctoral work at NIMTE. His research interests include the areas of lanthanide ion doped optical upconversion nanoparticles and their bioimaging application.

Aiguo Wu

Prof. Aiguo Wu received his PhD from Changchun Institute of Applied Chemistry, Chinese Academy of Sciences in 2003. After the postdoctoral stage at the University of Marburg, Germany and the California Institute of Technology, Pasadena, USA, he took up his research at Northwestern University, Chicago, IL, USA as a research associate. He is a professor since 2009 and has authorized over 330 SCI publications which have been cited more than 19 300 times with a H-index of 67. Prof. Wu's research area is primarily focused on the application of nanomaterials in biomedical, bioanalytical chemistry, and environmental sciences.

Fang Yang

Fang Yang is the master supervisor as well as an associate professor at the NIMTE. He received bachelor's and master's degrees in Physics and PhD in Physical Chemistry from the University of Marburg, Germany. He is currently a member of Youth Innovation Promotion Association of CAS, international members of the European Cooperation in Science & Technology (E-COST) and of the Action CA19118 ESSENCE program. He is committed to the development of functional nanomaterials, their physical and chemical properties and biological applications. he has published more than 50 SCI papers, including Nano Today, Biomaterials, Materials Horizons, ACS Nano, Angewandte Chemie, etc.

gained important attention, given its unique advantages: such as high spatiotemporal selectivity, low invasiveness, and low side effects.[8–10] The cytotoxicity of PDT is restricted to light-exposed regions harboring the photosensitizers, with the light used in PDT being non-harmful by itself. PDT is thus capable of selectively destroying malignant cells, while sparing healthy ones,[11] as long as efficient cancer cell targeting strategies are implemented to ensure the accumulation of PDT probes in pathological cells, keeping them out from healthy ones. The side effects of PDT are thus minimal compared to those of radiotherapy and chemotherapy.[12–14]

According to high-profile research databases such as Web of Science or Scopus the number of PDT-related research articles has been increasing in a yearly trend. The main topics of research covered in PDT-related articles revolve around: novel photosensitizers, mechanisms of operation, clinical applications, or synergistic combination of PDT with other therapeutic routes. In some of the most prominent working mechanisms of PDT, reactive oxygen species (ROS) are generated *in situ* in large quantities when photosensitizers are exposed to excitation light, in a wavelength range that is optimal to activate the PDT probe. Although ROS in low levels play an important role in supporting cellular life cycles, such as cell proliferation and homeostasis, thereby protecting our bodies from harmful factors such as microbial invasion, an imbalance between ROS generation and detoxification results in oxidative stress, leading to oxidative damage to biomacromolecules (*e.g.*, proteins, lipids, and DNA), or to inducing cell death mechanisms such as apoptosis, or necrosis.[15] Compared to normal cells, some cancer cells, especially those in advanced stages, are more dependent on antioxidants for cell survival and more vulnerable to exogenous ROS or compounds that weaken the antioxidant systems.[15] This concept of inducing preferential death of cancer cell was proposed two decades ago, and it is worth noting that ROS-mediated cell killing strategies are typically known to cause more damage to malignant cells than to normal cells due to differences in their redox states. Therefore, fighting cancer cells by exogenously-induced ROS has been considered a highly effective therapeutic strategy in diverse fields, such as immunology,[14,16–20] dermatology,[21–23] ophthalmology,[24] pneumology[25] and others.[26] Overall, a large body of PDT-related literature covers the development of chemical and technology-enabled photosensitizers that enhance ROS production as means to combat cancers.[27–29]

Conventional photosensitizers can be activated by short wavelength light (visible light, 400–700 nm),[30–33] and have been successfully applied to superficial cancers, such as for skin and esophageal tumors. However, targeting deeper tumors is still challenging. Specific laser excitation, falling in the photosensitizer's absorption band, is required for this to induce its therapeutic effects. As the excitation light is higher in wavelength, less tissue absorption and scattering occur, achieving thus higher penetration. The success of the therapy is also intimately intertwined with other properties of the incident light, which directly determine the effectiveness of the tumor treatment. For example, if a high energy single wavelength laser can be used, the duration of irradiation can be reduced, and the side effects of the treatment process can be relatively minimized. However, energy and wavelength are inversely proportional: as the wavelength increases, the energy decreases, and *vice versa*, so tuning the absorption band of the PDT probe is always a matter of compromise.

Photosensitizers operating with near-infrared light (NIR, 700–1700 nm) have attracted considerable attention in the context of biomedical applications. Most photo-thermal therapy (PTT) studies still focus on light in the NIR-I (700–1000 nm) biological window, and although the typical depth of NIR-I light penetration (1–3.5 mm) is slightly better than that of UV-visible light (1 mm), it is still significantly lower compared to the right end of the NIR-II window (1000–1700 nm), which allows penetration depths of up to 20 mm.[34] In addition, tissue autofluorescence is considerably reduced for the NIR-II window, while maximum permissible exposure is higher. Therefore NIR-II light is the more preferred source for PDT, especially for the treatment of deep-seated tumors. By now, several previous reviews have summarized the applications and limitations of PDT,[35–37] along with proposed formulations and utilizations of photosensitivers.[38,39] However, very few of these works have placed focus on NIR-II-driven photosensitizers and on associated PDT-based strategies for oncology. This review aims to address this gap, by overviewing recent important efforts in the field of nanomaterials-based PDT. After we first focus on the basic principle of PDT, we discuss various nanoparticle-shaped photosenzitizers, like traditional organic molecules, noble metals, upconversion nanoparticles, or carbon-based nanomaterials, highlighting how they have been applied in PDT. We further place focus on the integration of NIR-II photosensitizers with other therapeutic modalities, elaborating on the advantages of the combination of complementary therapies (Fig. 1). Finally, the existing challenges of photosensitizers based on NIR-II light activation are discussed, along with potential avenues to overcome these. In particular, we consider this review to represent a useful resource for those interested in a glimpse on the state-of-the art on NIR-II-driven PDT for the treatment of deep-seated tumors, with potential to stimulate further trains of thought followed by the development of more efficient technologies, capable to overcome the current limitations of NIR-II PDT.

2. The basic principles of PDT

Photosensitizers are converted from the ground state (S_0) to an unstable singlet excited state (S_n) when irradiated with an appropriate light as shown in Fig. 2. A fast internal conversion (IC) process then follows, which ends with the energy positioning at the lowest singlet excited state (S_1). The excited photosensitizer changes from the S_1 state to the triplet state (T_1) through intersystem crossing (ISC) for energy stabilization. According to the photochemical reaction processes taking place, two types of PDT have been reported.[36,37,40] In type-I reaction, T_1 reacts directly with the surrounding substrates to

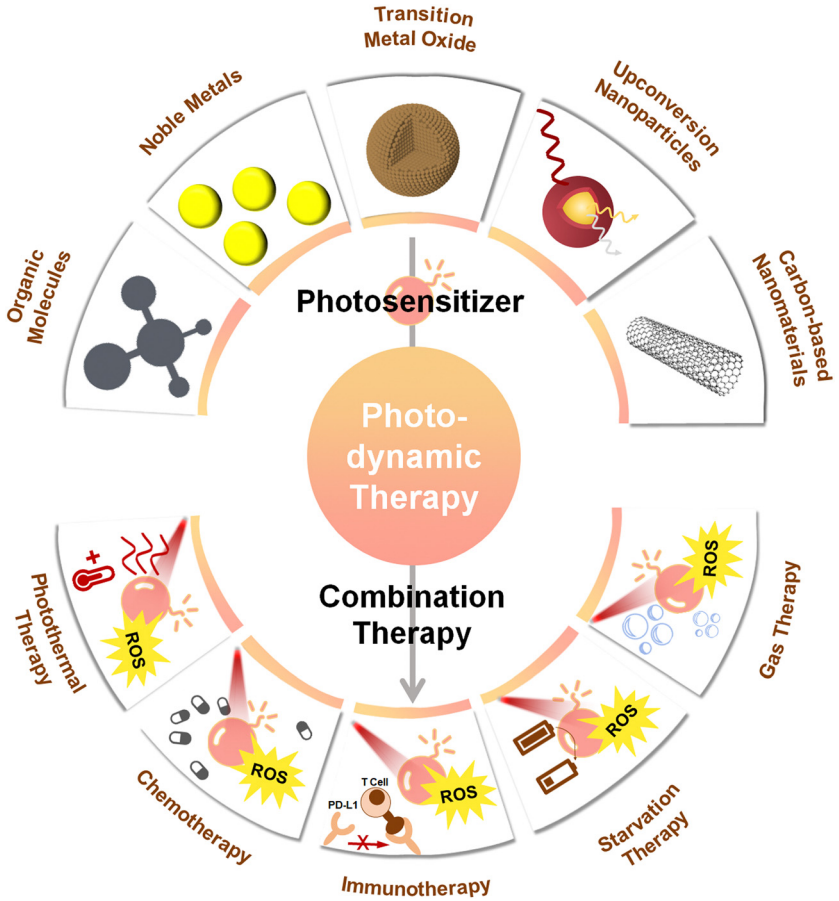

Fig. 1 Scheme of photosensitizers and photodynamic therapy activated by NIR-II light.

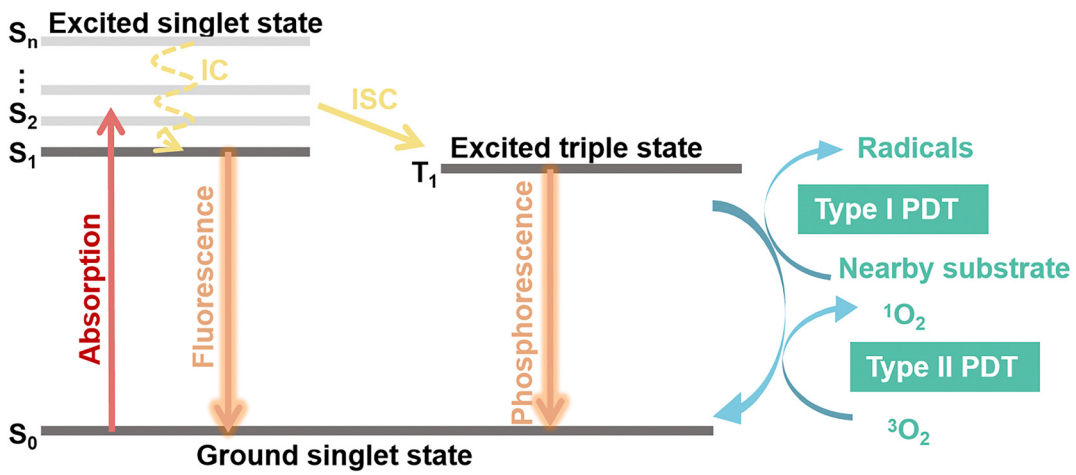

Fig. 2 The basic principles of type I and type II photodynamic reactions.

produce superoxide anions ($^{\bullet}O_2^-$) and hydroxyl radicals ($^{\bullet}OH$). In type-II reaction, the energy is transferred from molecular oxygen ($^3O_2$) to singlet oxygen ($^1O_2$), followed by reactions with biological molecules, which results in destruction of cancer cells. Type I and Type II PDT usually occur simultaneously, and the extent of the reactions is mainly dependent on the type of photosensitizers as well as the substrate and O_2 concentration.[38] An excess of ROS produced during PDT will attack surrounding macromolecules such as nucleic acids, proteins or lipids. The latter, especially unsaturated lipids, easily react with ROS to form lipid peroxides, which cause damage to bio-membranes.[41] Furthermore, these radicals

Table 1 NIR-II light-activated photosensitizers for cancer therapy

Category	Photosensitizers	Laser	Power	*In vivo* anti-cancer effect	Ref.
Traditional organic molecules	pTBCB-PEG	1064	1 W cm^{-2}	Hybridized semiconductor nanoenzymes with high photothermal conversion efficiency achieve PDT along with deep ablation and inhibition of metastasis	34
	SQ NPs	1150	0.1 W cm^{-2}	SQ NPs have excellent •OH generation capacity under hypoxic conditions	49
	TPBPy	1000	10 J cm^{-2}	Act as a mitochondrion-anchored photosensitizer for deep tumor tissues	50
Noble metals	Pd@Au-PEG	1064	1.3 W cm^{-2}	Core–shell nanostructures enhance the catalysis to produce O_2 for relieving tumor hypoxia	31
	AuNBP@CuS	1064	1 W cm^{-2}	The photoexcited plasmonic energy in the plasmonic metal is transferred to the semiconductor to enable immune responses	51
	Ag@Pd NCs	1270	1 W cm^{-2}	The presence of abundant active sites for catalytic reaction in the alloy nanostructures improve their peroxidase-like reaction kinetics	52
Transition metal oxide	Fe_3O_4/Ag/Bi_2MoO_6	1064	1 W cm^{-2}	Cascading nanocatalytic reactions achieve interactive, continuous, self-replenishment, so as to address the inefficiency and unsustainability of cancer therapies	53
	MoO_2	1064	1 W cm^{-2}	Photodynamic mechanism prompted by the LSPR photothermal effect, realizing significantly enhanced PDT at cellular level	54
Upconversion nanoparticles	Ln@Fe NPs	1064	0.6 W cm^{-2}	LnNPs act as energy converters for photoreduction of Fe^{3+} to Fe^{2+} enabling PDT in deep tissues	55
	UCNPs	1532	—	The crystal phase, size and emitting color can be easily manipulated, achieving 1532 nm light-triggered deep tissue bioimaging and PDT	56
	GNSGHs	1064	1 W cm^{-2}	The presence of fluorescence resonance energy transfer and double-site absorption in the NIR region contribute to the efficacy of PDT for deep tumor lesions	57
	UCNP/RB,Ce6-PEG	1550	0.5 W cm^{-2}	The upconversion emission of UCNP/RB,Ce6-PEG activates RB and Ce6, respectively	58
Carbon-based nanomaterials	CD@Nb_2 C	1064	0.4 W cm^{-2}	Heterogeneous junction induces accelerated carrier transfer, accompanied by GSH depletion and relief of hypoxic tumor	59
	Ti_3C_2/TiO_2-PVP HJs	1064	1 W cm^{-2}	The HJs still have a good ability to kill tumor cells at a depth of 5 mm when exposed to 1064 nm laser	60
	CD/TiCN HJ	1064	0.8 W cm^{-2}	Heterogeneous structure improves carrier transfer rate ultimately increasing ROS yield	61
	Ti_3C_2-Cu-PEG	1064	1 W cm^{-2}	Synergistic GSH depletion and photothermal enhancement of nanodynamic therapy	62

trigger free-radical chain reactions, resulting in oxidation or direct cross-linking modification of some amino acid sites of proteins. Following this chain of events, the protein's structure, catalytic activity, and biological functions are ultimately destroyed. Importantly, DNA is also sensitive to ROS in PDT.[42–44] To date, several studies have reported that Type II PDT dominates the photodynamic process because of its lower excitation energy requirement, despite the fact that it requires the consumption of abundant O_2 and thus severely affects the treatment and prognosis of tumors.[45–47]

3. NIR-II photosensitizers

The performance of the photosensitizers directly determines the efficiency of the PDT. Since the approval of photoporphyrin for clinical PDT treatment in 1993, the enhancement and optimization of the performance and function of photosensitizers has always been a hotspot of international cutting-edge research.[11,48] To date, about 20 photosensitizers have reached a sufficient technology readiness level to be commercialized or used in clinical trials. However, most of the currently available PDT regimens can only be used for superficial tumor treatment, with mild effect on deeper tumors, in best cases, which confines the number of clinical applications based on PDT[36] to a very limited segment of use scenarios. Over recent years, the development of novel nanophotosensitizers integrating: high $^1O_2$ quantum yield, active targeted delivery, tumor specificity, and deep treatment, has become a worldwide priority. NIR-II light features deeper penetration depth and lower scattering, compared with NIR-I light, and thus strong focus has been placed on the formulation and application of NIR-II-driven photosensitizers.

In this section, instead of attempting to cover all photosensitizers activated by NIR-II light, we focus on some of the most widely studied organic and inorganic nanomaterials, including noble metals, upconversion nanoparticles, transition metal oxides, and carbon-based nanomaterials, summarized in Table 1.

3.1. Traditional organic molecules

The first generation of organic photosensitizers was comprised of porphyrin and porphyrin derivatives. In 1976, Kelly *et al.*[48] initiated the first PDT clinical trials on humans using a haematoporphyrin derivate (HPD) to slow the tumor growth and finally to induce the tumor necrosis. As a result, HPD-based photosensitizers were finally approved for bladder cancer in Canada.[63] Then, in order to improve the drawbacks of these photosensitizers, such as low tissue penetration, reduced ROS production, or high retention time, macrocyclic compounds composed of porphyrin were developed. These compounds

feature higher quantum yields, compared to porphyrin's. Furthermore, they can be activated by light of longer wavelengths, which means these photosensitizers could be applied to deeper tumors. However, most porphyrin and porphyrin derivatives can be activated by UV and visible light in the range of ~400–700 nm,[9,14,64–66] which has important disadvantages compared to light in the NIR-II window, as discussed earlier. Later, several conventional organic molecules, such as squaric acid and cyanine dyes, have been developed as NIR-II photosensitizers.[49,67–69] Peng's group discussed functional systems of specific targeting cyanine structures for accurate tumor diagnosis and therapy,[70] and designed a variety of longer wavelength absorbing and emitting eukaryotic dyes.[68,71]

Since Tang's discovery of the aggregation-induced emission (AIE) properties in 2001, that is, AIE-characterized molecules exhibit unique luminescence-enhancing properties due to the limitation of the molecular movement in the aggregated state,[72] more and more studies have reported on to use AIE molecules as PDT photosensitizers.[50,73,74] The main reason for this, as analyzed by Tang's group,[75] is their high ability to generate photo-triggered ROS in the aggregated state. Both Cheng's[76] and Liang's[77] teams demonstrated that benzothiadiazole molecules connect to strong electron donors to lower the energy gap and optimize acceptor–donor–acceptor–donor–acceptor (A–D–A–D–A) scaffolds, which was important to elucidate the relationship between steric-hindrance effects and optical behaviors. Specifically, the construction of twisted conformations of D–A systems with large dihedral angles limits the intramolecular rotation. It establishes a molecular design strategy based on the steric-hindrance effect to yield NIR-II photosensitizers that not only achieves a significant enhancement of the twisted intramolecular charge transfer emission efficiency,[78] but also maintains the excitation energy for $^1O_2$ generation.[79] Based on this, Xiao *et al.*[79] proposed a molecular design strategy for an A–D–A–D–A type of AIE photosensitizer, BNET, by modulating the steric hindrance of molecules. This nearly vertically twisted design strategy enhanced the NIR-II region emission peaks of the photosensitizer in the aggregated state while maintaining sufficient excitation energy to generate $^1O_2$.[80,81] In orthotopic colon or pancreatic tumor model, BNET demonstrated good PDT performance (a complete cure without recurrence in 60 days). It is important to mention though that, unlike the previous example, the majority of AIE molecules absorb and emit in the visible light region, which severely limits their practical application in deep-tissue therapy.

While traditional photosensitizers require the absorption of a single photon equal to the energy of the bandgap, two-photon excitation involves the photosensitizer absorbing two lower-energy infrared photons, thereby increasing the penetration depth of PDT and decreasing photo-bleaching of the photosensitizer (ineffective oxidation owing to multiples factors).[82] Such strategies feature an additional advantage, namely, the spatial localization of the pulsed laser required for the excitation of the two-photon PDT is more precise, because the high-intensity irradiation is produced only at the focal point.[83–85] A relevant example stands in the work of Luo and his colleagues,[50] who synthesized an AIE photosensitizer with NIR-I emission, namely TPBPy, encapsulated in liposomes, that was used for fluorescence imaging-guided two-photon PDT. Under fs-laser excitation (1000 nm), TPBPy exhibited strong NIR-I fluorescence in multicellular tumor spheroids, with an imaging depth of 210 μm, which was significantly superior to single-photon excitation. In addition, TPBPy was found to be very effective in producing $^1O_2$, inhibiting tumor growth under NIR-II light irradiation.

3.2. Noble metals

Ever since the advent of nanotechnology, a series of nanomaterials have been reported to exhibit an efficient ROS generation ability, enabling their use as photosensitizers in PDT.[12] Among them, noble metal nanomaterials have attracted worldwide attention owing to their unique optical, electrical, magnetic, thermal and mechanical properties. In current days, important efforts have been placed on modulating the localized surface plasmon resonance (LSPR) effect by changing the composition, morphology, and structure of noble metals. Such strategies can also be used to achieve strong absorption in the NIR region, which promote noble metals as highly useful tools for implementing high-end applications in biomedicine, including in diagnostics, therapy and theranostics.[31,51,86] Among these, gold nanomaterials feature very convenient properties, such as simple preparation and modification, high biocompatibility and excellent chemical stability, making them one of the main candidates to be considered for clinical therapeutic applications.[87] Since the formulation of gold nanoparticles by Faraday in 1847, gold nanomaterials employed in the field of PDT have been gradually developed and studied.[31,88]

An effective approach to improve the PDT efficiency of gold nanomaterials, stands in finely tuning their size and morphology. This applies to nano-structures of various types, ranging from the most explored morphologies (sphere,[89] ring,[90] rod,[86,91] and nanoclusters[92–94]) to special structures (nanostars,[95,96] nanoprisms,[97] nanovesicles,[98] and gold nanobipyramids).[51,99–101] Yuan's group[102] synthesized and explored the effect of different gold nanoparticles' size (6.2–61.2 nm) on their biodistribution and cytotoxicity (Fig. 3a). An important finding of this study was that small gold nanoparticles (Au NPs), with large specific area, exhibit higher PDT efficiency given the higher number of sites for nanoparticles to interact with the biomolecules. Another finding was that small-sized Au NPs could accomplish broader biodistribution and were nearly metabolized within 30 days, whereas a large fraction of large-sized Au NPs were found to remain in the liver and spleen at 90 days (poor elimination rate) as shown in Fig. 3b. These results were highly meaningful for the subsequent clever design and successful application of Au NPs in the biomedical field.

In another study, Zhang *et al.*[103] compared the photoactivities of gold nanomaterials with different morphologies, namely Au nanorods (Au NRs), nanoshells (Au NSs), and nanocages (Au NCs) (Fig. 4a). As well known, hot electrons

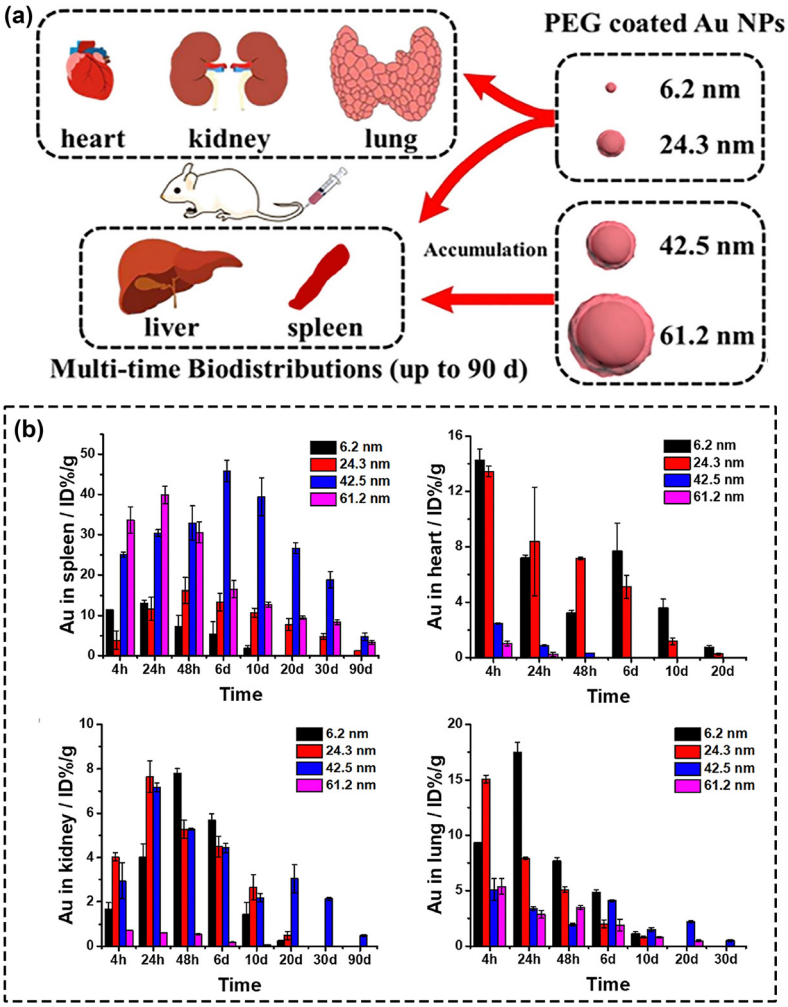

Fig. 3 (a) Schematic assessment of size effect on biodistribution and cytotoxicity of AuNPs. (b) The biodistribution of different-sized Au NPs. Reproduced with permission from ref. 102. Copyright 2018, Elsevier.

can be generated due to the plasma-induced electric field in noble metal nanostructures, and the hotter the electric field, the higher number of hot electrons (Fig. 4b). By comparing the electromagnetic field distribution profiles of these three nanostructures, Zhang *et al.* found the presence of electric field on both the inner and outer surfaces of Au NCs, which leads to the emergence of electric dipoles (Fig. 4c). Moreover, the study found that the generated electric dipoles can also sensitize oxygen to form ROS through energy and electron transfer modes, ultimately exhibiting photodynamic properties.[104]

The teams of Cai[105] and Zhang[106] reported multifunctional nanoplatforms based on gold-based nanomaterials modified with a peptide RLA and hyaluronic acid, respectively. When exposed to NIR light, these nanoplatforms not only induced the generation of ROS through the localized electric field of gold nanomaterials but also enhanced PDT effectiveness by facilitating tumor-targeting-mediated accumulation of endogenous ROS. As mentioned before, the efficient generation of high-energy hot carriers from the LSPR of noble metal nanomaterials stands at the core of LSPR-based PDT. In this context, it is important to highlight that alloying represents a widely used strategy to tune the LSPR of metals, so as to achieve the optimization of their optical properties.[107] A relevant example in this field is the work of Zhang *et. al.*,[31] who developed two-dimensional Pd@Au bimetallic core–shell nanostructures (Fig. 5a and b) and investigated the effect of modified LSPR on the ability of the therapeutic agent to generate dissolved oxygen (Fig. 5c and d). Another relevant example is the work reported by Wang's team,[52] who prepared DNA-templated Ag@Pd alloy nanoclusters exhibiting photoresponsive properties under 1270 nm laser irradiation. They demonstrated that the combination of Pd with Ag not only alters the LSPR of the metallic composite but also significantly increases the absorbance cross-section, thus providing more catalytic active sites to generate large amounts of ROS (Fig. 5e). Gold-based nanohybrid materials leverage the characteristics of various materials to achieve adjustable or synergistic enhancement of the optical properties of the gold-based nanocomposite, thereby overcoming the constraints associated with individual components. For example, the teams of Jiang[108] and Hang[51]

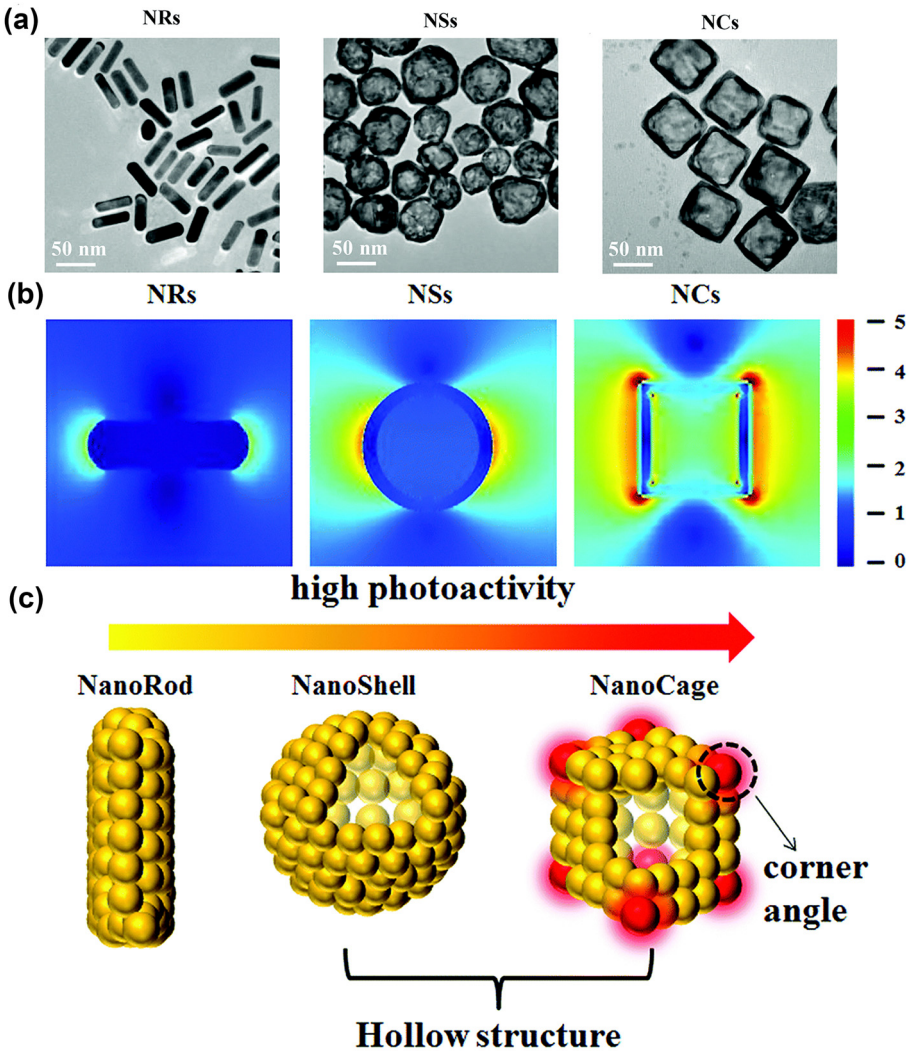

Fig. 4 (a) TEM images of Au NRs, NSs and NCs. (b) The electric field distribution and enhancement ($|E|/|E_0|$) contours of Au NRs, NSs and NCs. (c) Illustration of the photoactivity of Au nanostructures. Reproduced with permission from ref. 103. Copyright 2018, The Royal Society of Chemistry.

constructed multifunctional semiconductor nanocomposites by coating gold nanobipyramid (Au NBP) with cuprous oxide (Cu_2O) and copper sulfide (CuS), respectively. They both demonstrated in *in vivo* and *in vitro* studies that, in addition to the strong LSPR peak and narrow half-peak width, due to the unique pentagonal base and two sharp apexes of Au NBP,[109] the construction of semiconductor composite structures based on Au NBP could achieve effective separation of electrons and holes, thereby promoting ROS generation.

3.3. Transition metal oxide

Besides noble metal nanomaterials, in recent years transition metal oxide nanomaterials have also received important attention in the context of PDT, given their superior biocompatibility and tunable LSPR effects.[54] Transition metal oxides, including TiO_2,[110] ferrite nanomaterials,[111–114] MnO_2,[115–117] Cu_2O,[118] *etc.*, are currently regarded as some of the most popular biomedical materials given their low-cost, high bioactivity, good biocompatibility, and higher chemical stability than noble metals.

The introduction or direct functionalization of transition metal oxides represented an important advance in the context of flexible platforms for tumor diagnostics and therapeutics. By such strategies, the generation of ROS can be accomplished in several ways.[88,119] On one hand, transition metal oxides form distinctive defects due to the ionicity of the meta-oxygen bond and different degree of orbital mixing or hybridization.[120] Therefore, by functionalized transition metal oxides, the modulation of oxygen vacancies regulates the bandgap or surface electron distribution, helping optimize the photocatalytic performance of the nanomaterial.[121,122] Xu *et al.*[123] narrowed the band gap of MoO_3 through hydrogenation-regulated oxygen vacancies engineering for NIR-II-excited photonic hyperthermia-enhanced catalytic therapy. Ge *et al.*[124] fabricated heterojunctions of g-C_3N_4/Bi_2MoO_6/Bi to accelerate carrier transfer, resulting in highly enhanced photocatalytic performance. Based on the oxygen vacancy regulation strategies of molybdenum oxides and the properties of heterojunctions, Dong's team[53] designed Bi_2MoO_6 NP (BMO NP) doped with

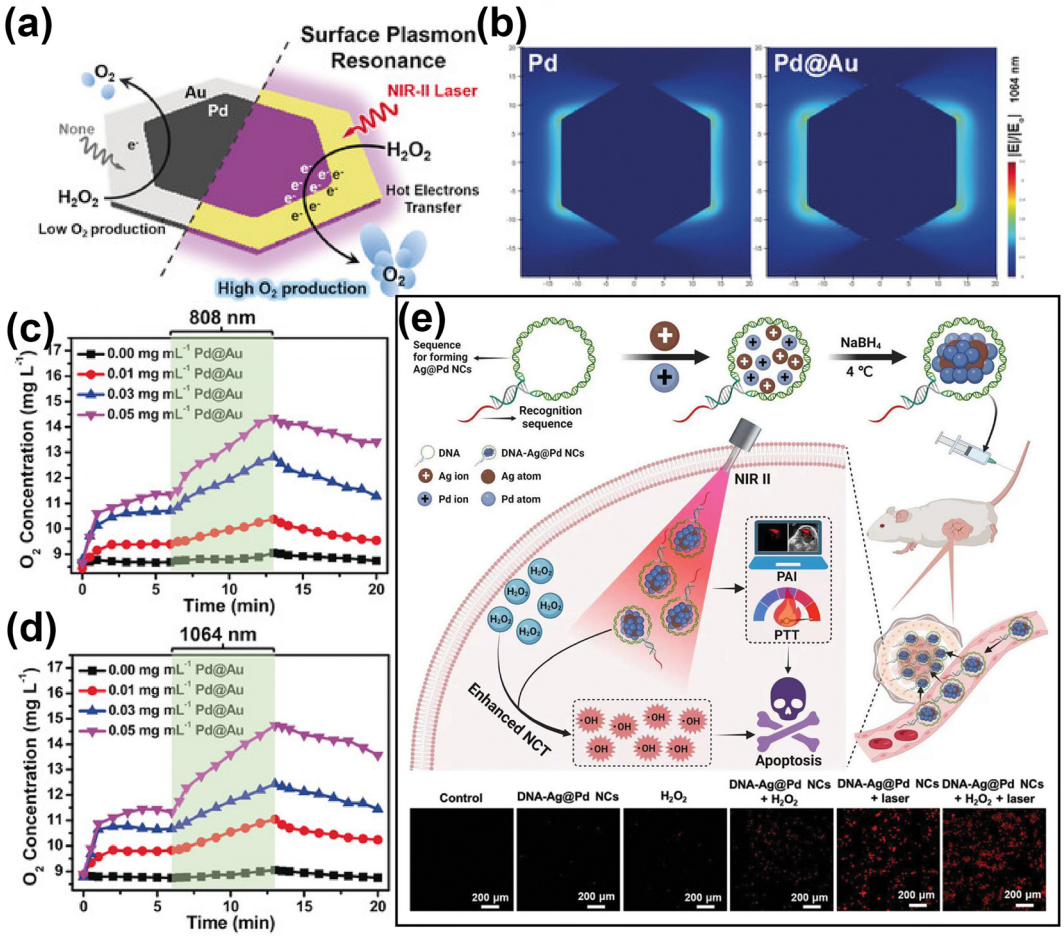

Fig. 5 (a) Illustration of Pd@Au for rapid increase of O_2 concentration under NIR laser irradiation *via* surface plasmon resonance effect. (b) Comparison of electric field enhancement ($|E|/|E_0|$) contours of bare Pd and Pd@Au at 1064 nm excitation. (c) and (d) The O_2 concentration of H_2O_2 incubated with different concentration of Pd@Au and under irradiation by 808 or 1064 nm laser irradiation. Reproduced with permission from ref. 31. Copyright 2019, Wiley. (e) Schematic illustration of DNA-templated Ag@Pd alloy nanoclusters-based synergetic therapy and the generation of ROS in different treatment groups. Reproduced with permission from ref. 52. Copyright 2023, Wiley.

Fe_3O_4 and Ag NPs to endow the composite nanomaterial with strong NIR-II absorption properties, which greatly enhanced the photocatalytic activities. As shown in Fig. 6a, this photoactivatable "all-in-one" nanoparticulate system enables electrons enriched in the conduction band of the BMO NP to cycle and migrate between BMO NP, Fe_3O_4 and Ag NPs. The introduction of impurity energy levels significantly narrows the effective bandgap, thus transforming the absorbed light into the NIR II region. Fig. 6b and c illustrate the performances of this nanoplatform to achieve sustainable, self-replenishing, ROS yield, driven by light through multiple forms of free electron enrichment.

On the other hand, significant endeavors have demonstrated that employing transition metal oxides can establish a cascade reaction platform, addressing the inherent limitations of PDT and enabling the adoption of a double- or triple-punch strategies that enhance the effectiveness of cancer treatment.[115] In this context, it is important to recall that the tumor microenvironment (TME) acts as the "soil" on which tumors thrive. The demanding metabolism of tumor cells leads to the presence of unique features of TME including hypoxia, acidity, and glutathione (GSH) overexpression.[125,126] Therefore, the development of TME-activated nanodiagnostics and therapeutic integration is highly attractive for precision cancer medicine. The existence of transition metal oxides can be likened to a switch that solely activates in TME, thereby minimizing side effects on normal tissues while creating an optimal response environment to enhance PDT efficacy.[127] Wang's group[115] constructed a multifunctional nanoplatform, MUM NPs, consisting of AIE-active free radical photosensitizers, MnO_2, and upconversion nanoparticles (UCNPs). The UCNPs enabled AIE photosensitizers to be activated by NIR light to produce $^{\bullet}OH$, and the MnO_2 shell was "turned on" by the high level of intracellular GSH to produce Mn^{2+}, which not only achieves a rapid GSH depletion to increase intracellular ROS, but also converts H_2O_2 to $^{\bullet}OH$ in the form of Mn^{2+} *via* a Fenton-like reaction (Fig. 7). Likewise, Zhang *et al.*[128] demonstrated an omnipotent nanoplatform MnO_2/Ag_3SbS_3 for TME-responsive PDT, where MnO_2 not only provided enhanced PDT, but also protected the small-sized Ag_3SbS_3 from early metabolization due to the degradation

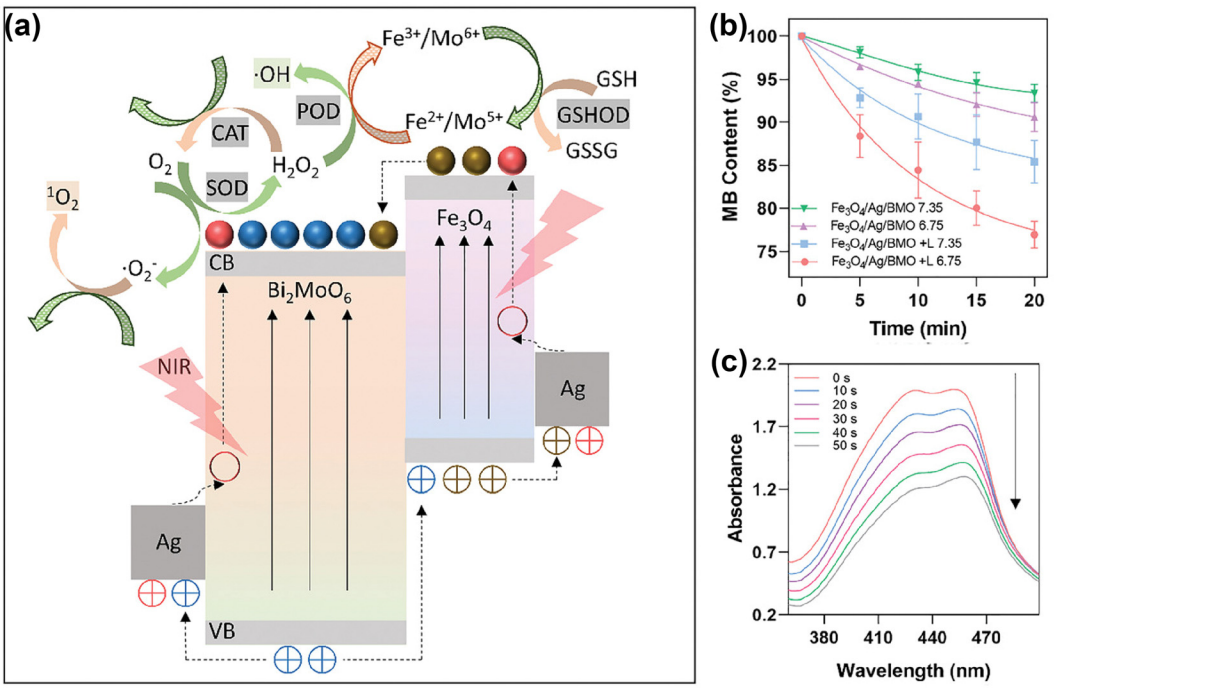

Fig. 6 (a) Schematic illustration of the working mechanisms underlying the intraparticulate interactions of BMO NP. (b) Degradation of MB for •OH generation. (c) Light adsorption of DPBF decreases due to $^1O_2$ generation under laser irradiation with different durations (0–50 s). Reproduced with permission from ref. 53. Copyright 2021, Wiley.

of MnO_2 by the acidic environment. In addition to MnO_2, Zhao's group[129] reported that the hollow-structured MoO_x NPs have strong NIR light absorption, confirming that the optical properties of MoO_x NPs can be modulated by changing their chemical composition. Later, they reported plasmonic PEGylated molybdenum oxide nanoparticles (PEG-MoO_x NPs) that absorb both 808 nm and 1064 nm light.[130] Interestingly, PEG-MoO_x NPs could only perform limited PTT under 808 nm light irradiation, whereas under 1064 nm light irradiation the PEG-MoO_x NPs were able to perform both PTT and PDT.

3.4. Upconversion nanoparticles

Upconversion nanoparticles (UCNPs) are usually composed of host lattices of ceramic materials doped with lanthanide or actinide ions, and their unique optical properties are primarily associated with the ability to emit at short-wavelength, typically in the visible, when irradiated with long wavelength, usually in the NIR.[131,132] In comparison to other photosensitizers, UCNPs feature two important advantages: (a) their emission band can be tuned so that overlap with autofluorescence can be avoided,[133] and (b) NIR excitation allows high penetration depth.[134] The great majority of UCNPs exhibit: small size, intense visible emission, sharp emission bandwidth, long luminescence lifetime, high photostability, and low cytotoxicity. Such excellent properties render UCNPs a highly convenient solution for applications in bio-sensing,[135] bioimaging[136,137] and cancer therapy.[55,138–140]

When applied in PDT, UCNPs can be used as agents that convert NIR light to higher-energy light for the efficient activation of photosensitizers and as photosensitizers themselves. With respect to the first part, Yeh *et al.*[58] proposed a dual-photodynamic strategy to boost the generation of $^1O_2$ (Fig. 8a). Among trivalent lanthanide ions, Erbium ions (namely Er^{3+}) provide possibilities for multi-peak upconversion luminescence (UCL). This can be used to initiate a range of activators upon NIR-II light irradiation. In this nanoplatform, the dual photosensitizers, rose bengal (RB) and chlorin e6 (Ce6), were excited respectively by the green and red emission from UCNPs to generate an abundant amount of $^1O_2$ under 1550 nm laser irradiation. Briefly, the green (~550 nm) and red (~670 nm) emission of UCNPs overlapped with the absorption peaks of RB and Ce6 respectively, so that a sharp decrease in the green emission of UCNPs/RB and the red emission of UCNPs/Ce6 occurred under irradiation at 1550 nm (Fig. 8b–d). Xu *et al.*[138] not only took advantage of UCL of Er^{3+}, but also boosted the downconversion emission of Er^{3+} by the cross-relaxation effect of Er^{3+} and Ce^{3+} ions in order to expand the excitation threshold of Fe/Mn-ZIF-8. Although the therapeutic efficiency of PDT is limited due to the restricted energy available for the conversion of UCNPs to photosensitizers, a number of studies published in the literature have demonstrated significant efficiencies of coupling UCNPs with other materials. Recently, in order to better utilize the emission energy of Er^{3+}, Liu's team[141] designed and developed UCNPs with a multilayer structure to concentrate the emission (energy transfer efficiency near 60%) with high efficiency; Li's team[140] encapsulated an organic photosensitive molecule in multilayer structured UCNPs to amplify NIR-triggered PDT efficiency in

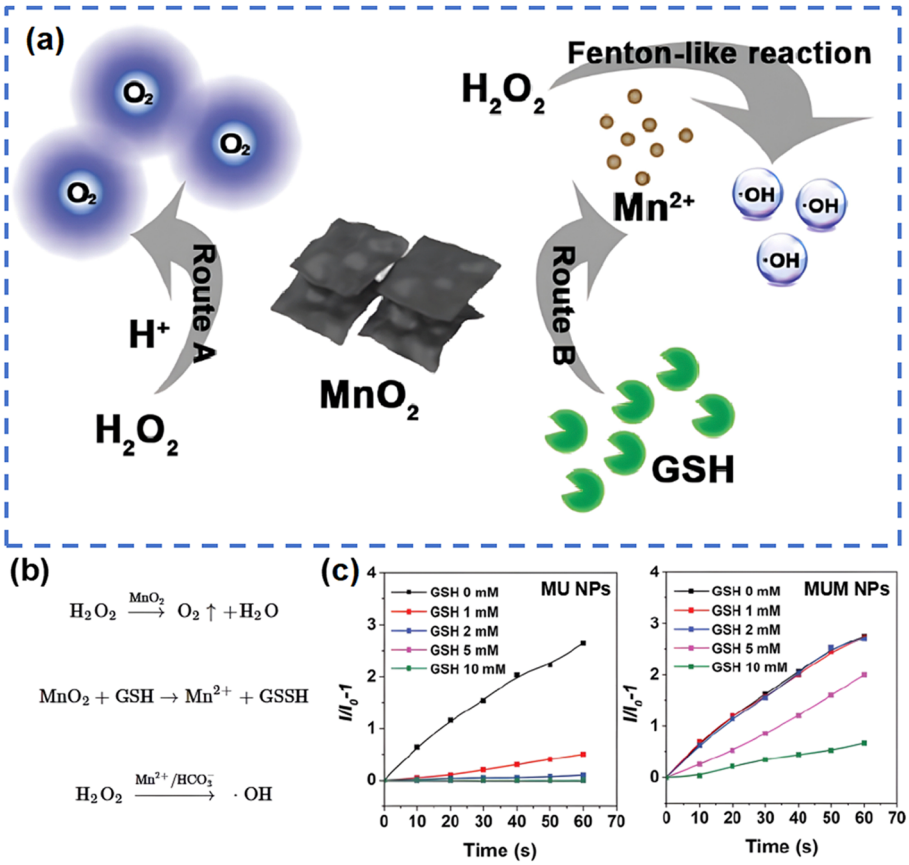

Fig. 7 Schematic pathways (a) and equations (b) for GSH decomposition and •OH production by MnO_2 in MUM NPs. (c) The generation of •OH of MU NPs and MUM NPs under different GSH concentrations, indicated by HPF (a fluorescent probe specifically responsive to •OH). Reproduced with permission from ref. 115. Copyright 2021, Wiley.

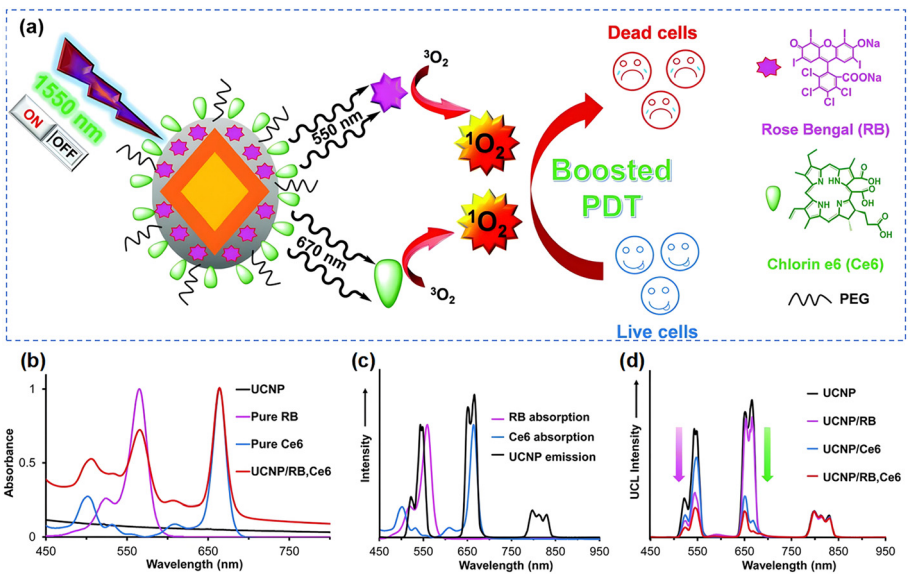

Fig. 8 (a) Schematic diagram of the formation of UCNP@SiO_2/RB,Ce6. (b) The absorbance of UCNP, RB, Ce6, UCNP/RB,Ce6. (c) The absorption and emission spectra of RB, Ce6 and UCNPs respectively. (d) The UCL spectra of UCNP, UCNP/RB, UCNP/Ce6 and UCNP/RB,Ce6 under irradiation at 1550 nm. Reproduced with permission from ref. 58. Copyright 2014, The Royal Society of Chemistry.

the hypoxic environment. With respect to the second part, Zhang and colleagues[110] fabricated a Yb/Er co-doped titanium dioxide nano-shovel/quercetin/L-arginine (TiO_2@UCN/Qr/LA) phototherapy platform. The doped rare-earth elements not only increased the absorption of TiO_2 in the near-infrared band but also produced abundant oxygen vacancies to prevent electron–hole pairs recombination, thus improving the photocatalytic performance. In another body of relevant efforts, to extend the excitation band of upconverted materials farther into the NIR-II region, Zeng and colleagues[56] constructed novel Er/Mn co-doped NIR-II photoresponsive UCNPs loaded with zinc phthalocyanine (ZnPc). Mn^{2+} ions provided two important features to this composite nanomaterial: (i) enhanced single-band red emission at 1532 nm, (ii) phase and size control, helping overcome surface defects. The UCL intensity tended to increase and then decrease when the Er^{3+} concentration was varied, and the nanomaterials changed from the coexistence of large-sized rods and small-sized cubes to highly monodisperse cubic nanoparticles when the Mn^{2+} doping amount was increased step by step. Additionally, the red UCL intensity was increased tenfold by adjusting the concentration of Mn^{2+} in the UCNPs.

3.5. Carbon-based nanomaterials

Carbon-based nanomaterials have extraordinary potential for implementing PDT applications owing to their ease of fabrication and modification, targeting capability, rich functional groups, great biocompatibility and low cost. Particularly, carbon dots and 2D transition metal carbide and nitride compounds (termed MXenes) have been used in recent years as the foundation for important biomedical applications such as bioimaging[142–144] or cancer therapy.[59,60,89,145]

Carbon dots (CDs), zero-dimensional carbon-based nanomaterials, are generally sized in the range of 1 to 10 nm, and have functional groups on their surfaces, including $–NH_2$, –OH and –COOH, which make them equipped with the ability to be further functionalized, while exhibiting great aqueous solubility, a highly important asset for biomedical applications. CDs have been widely employed as optical nanoprobes, with Rogach and his coworkers having made an important contribution in this regard by exploring the relationship between the absorption and emission wavelengths of CDs and their size.[146] In subsequent studies, by introducing electron-acceptor groups on the surface, they significantly enhanced the absorption and emission of CDs in the NIR region.[147] This was followed by an ingenious increase of the surface electron-acceptor groups on the π-conjugated cores to realize the red-shift of the main absorption band.[148] In the context of PDT, a recent study of interest is the work of Zhu *et al.*[59] who reported NIR-II-triggered CDs@Nb_2C nanozyme with triple enzyme mimetic activity. Complete tumor elimination was achieved by depletion of glutathione, alleviation of hypoxia and enhancement of ROS generation efficiency. The CDs in this composite nanomaterial could rapidly convert intracellular H_2O_2 to O_2 for alleviating tumor hypoxia, while attenuating the reductive nature of the TME by mimicking peroxidase (POD) and glutathione-peroxidase (GPX) to produce $^{\bullet}OH$. Following the creation of heterojunctions between carbon dots (CDs) and Nb_2C, the NIR-II irradiation prompted the transfer of excited electrons from the conduction bands of Nb_2C nanosheets to the valence bands of CDs due to the presence of an internal electric field. This phenomenon facilitated the electron transfer process, leading to an escalation in catalytic activity.

Another relevant family of carbon-based nanomaterials, MXenes, has been actively investigated since 2011.[149] Two-dimensional MXenes nanomaterials with nanoscale-lateral size and atomic-scale thickness can be obtained by selective etching the transition metal layer M (such as Ti, Zr, Hf, V, Nb, Ta, Cr, Mo and so on) in $M_{n+1}X_nT_x$. The MXenes exhibit robust light absorption properties covering the entire UV, visible and NIR regions,[150,151] showing great potential in light energy conversion. By functionalization, the photoabsorption properties of MXenes can be finely tuned, and by delaying the recombination of electrons and holes, ROS generation capabilities can be significantly promoted, hence greatly improving potential PDT effects.[12] Ti_3C_2, as a common MXenes nanosheet, is usually used to load drugs or other functional substances for combined tumor treatment due to its large specific surface area and facile modification.[152] A relevant effort to discuss is the work of He's group,[60] who manufactured a nanoplatform with MXenes heterostructures, *i.e.* Ti_3C_2 MXenes loaded with TiO_2 (Ti_3C_2/TiO_2 HJs), Fig. 9a. In this study, the band gap of Ti_3C_2/TiO_2 heterojunctions was positioned in between TiO_2 and Ti_3C_2, which allowed its absorption band to be tuned from ultraviolet for TiO_2 to the entire visible-NIR-II region (Fig. 9b). Fluorescence spectroscopy, Fig. 9c, showed that the transfer of photoinduced electrons to the surface, and finally the effective inhibition of carrier recombination, is attributed to the introduction of Ti_3C_2 MXenes. In other words, the excellent opportunity for ROS generation was provided by the simultaneous presence and interaction of NIR-II light and the heterojunction electron field. With Schottky junctions representing another specialized structure that relies on efficient separation of carriers, Zhang and his group[153] prepared a Schottky junction nanozyme with a narrow bandgap, and enhanced electron–hole separation. They demonstrated that Ti_3C_2 in Schottky junctions acted as cocatalysts to receive photoexcited electrons more efficiently, which effectively suppressed the recombination of photogenerated electrons and holes, and thus improved the NIR photocatalytic performance.

4. Combining therapy

While PDT has gained popularity as a therapeutic approach, it remains a dynamic and evolving process characterized by multifactorial interactions.[154] Currently, there is a lack of a quantitative and standardized description of the *in vivo* response processes associated to PDT in relation to the diverse photodynamics aspects. In addition, PDT approaches are limited by various factors, such as the location and size of the tumor, targeting precision,[155] and the high level of dependence of most photosensitizers on tissue oxygen concentration[38] (see

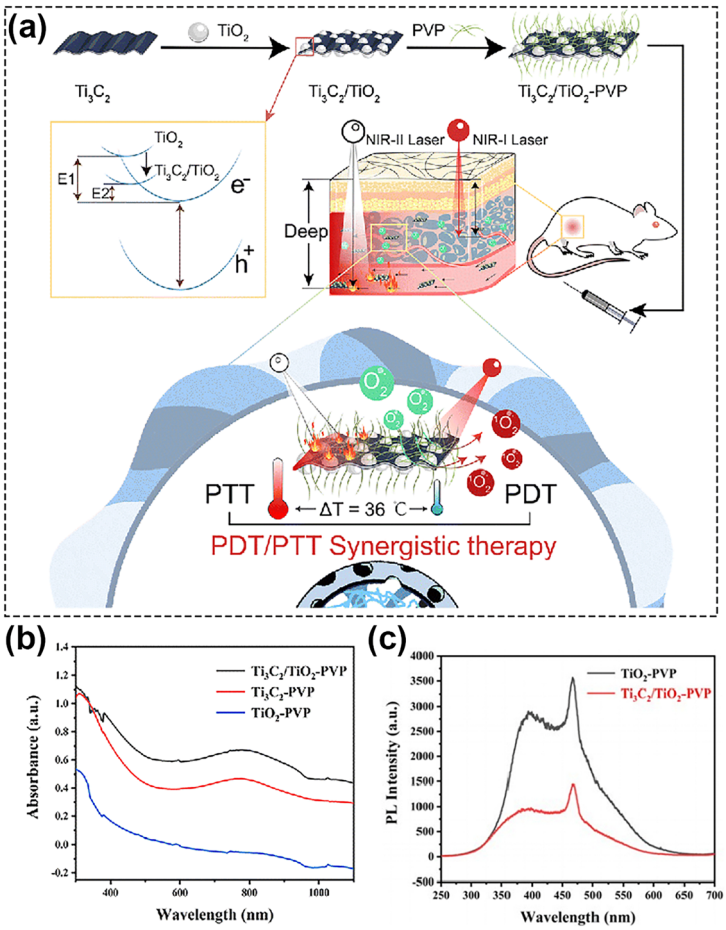

Fig. 9 (a) Schematic of NIR-II-triggered PTT/PDT therapy using Ti_3C_2/TiO_2 HJs. (b) The absorption spectra of TiO_2-PVP, Ti_3C_2-PVP, and Ti_3C_2/TiO_2-PVP. (c) The fluorescence spectra of Ti_3C_2/TiO_2-PVP. Reproduced with permission from ref. 60. Copyright 2022, The Royal Society of Chemistry.

Section 2). These factors contribute to inadequate therapeutic outcomes in numerous scenarios. A solution to overcome the limitations of PDT, stands in synergistically combining it with other therapeutic approaches, such as photothermal therapy (PTT), chemotherapy, immunotherapy or starvation therapy. Such combined approaches can yield better efficiency compared to any of the employed therapeutic solutions by itself (Table 2). In the next we will discuss past relevant efforts that were aimed at synergistically combining PDT with other therapeutic approaches.

4.1. Combining photodynamic therapy and photothermal therapy

Photothermal therapy (PTT) and photodynamic therapy (PDT) are two distinct types of phototherapy that differ in their mechanisms of action and employed agents: while PDT relies on the capacity of an interaction between a photosensitizer, light, and oxygen to produce ROS, which can cause cell damage and death, PTT involves the conversion of light energy into heat, that can selectively damage or destroy targeted cells or tissues. There is a large body of literature presenting various ways by which PDT and PTT can be jointly used, given their similar light activating condition.[61,170–173] Among these efforts, in a study[174] presented by Christensen and co-authors, a synergistic relationship between mild hyperthermia and PDT was demonstrated. Namely, it was shown that an increase in local temperature (41, 42.5, 45 °C) at cellular level represents a viable mean to sensitize cells to PDT. At the tissue level, the efficacy of conventional oxygen-dependent PDT in hypoxic tumor regions could also be improved by PTT.[158,175] In addition, previous studies have showed that the cytotoxicity of PTT can be further enhanced by additional ways such as the acidification of hypoxic tumor regions due to the Warburg effect (vigorous oxygen-consuming glycolysis[176]) present in PDT[177] and the destruction of heat shock proteins (HSPs) by ROS generated during PDT.[178] *In vitro*[179] and *in vivo*[172] studies conducted by Chen *et al.* demonstrated the specific mechanism underlying the synergistic enhancement of cell death and tumor growth control by aggravation of cancer cell necrosis and tumor vascular injury with hyperthermia immediately after PDT. Consequently, this synergistic treatment modality holds significant potential to achieve super-additive outcomes.

In the valuable work reported by Wang *et al.*,[156] the authors constructed FeS_2/CoS_2@PEG (FCs@PEG) Z-scheme nanoheterostructures (Fig. 10a). CoS_2 (1.37 eV) and FeS_2 (1.16 eV) represent n-typical semiconductors characterized by an interface

Table 2 Reported approaches that combine PDT with complementary therapies

Combination strategy	Photosensitizers	Laser (nm)	Power	Tumors	*In vivo* anti-cancer effect	Ref.
PDT combined with photothermal therapy	FCs@PEG NSs	1064	1 W cm^{-2}	HepG-2	Z-Scheme heterostructure enables efficient in-tandem PDT/PTT	156
	CeO_{2-x}@HA	1064	1 W cm^{-2}	4T1	given numerous oxygen defects, CeO_{2-x}@HA completely eradicates tumors without systemic toxicity	157
	BLICP@O_2	1064	1 W cm^{-2}	Huh7	Enhanced PDT for hepatocellular carcinoma by precisely controlling the release of oxygen through the photo-thermal effect to relieve tumor hypoxia	158
	DNA-Ag@Pd NCs	1270	1 W cm^{-2}	MKN-45	photothermal-augmented nanocatalytic therapy of gastric cancer.	52
PDT combined with chemotherapy	DOX- HMNCs	1064	0.8 W cm^{-2}	HeLa	HMNCs have pH-responsive drug release capabilities and the ability for precise generation of •OH	159
	CuS@PDA/Pd	1064	1 W cm^{-2}	4T1	NIR-II light accelerates the bioorthogonal reaction of CuS@PDA/Pd, and dual drug synthesis leads to improved therapeutic efficacy	160
	CS/Cu_{2-x}Se-TPZ NPs	1064	0.5 W cm^{-2}	4T1	Combination therapy of endogenous acidic micro-environment and exogenous NIR-II -triggered nanoprobes loaded with a hypoxic prodrug TPZ overcome hypoxic microenvironment hindrance	161
	NPD@M	1064	0.5 W cm^{-2}	U14	Plasma assemblies enable the reversion of multidrug resistance to improve chemotherapy and killing for deep tumor cells under NIR-II light exposure	150
	UF@PPDF NPs	1064	1 W cm^{-2}	4T1	Hierarchically assembled γ-Fe_2O_3 nanocrystals enable switchable magnetic resonance imaging and controlled release of iron ions and chemotherapeutic drugs	162
PDT combined with immunotherapy	AIPH@MS-CTPP	1064	1 W cm^{-2}	4T1	PDT of AIPH reprograms tumor-associated macrophages from the M2 to M1 phenotype	163
	Au/Ag nanorod	1064	1 W cm^{-2}	4T1	Au/Ag NRs in combination with ICB antibodies inhibit distant tumor growth and tumor recurrence	164
	Cu_8S_9	1064	0.2 W cm^{-2}	4T1	NIR-II laser-mediated plasmon-driven photoredox chemistry enhances the immune responses	165
PDT combined with starvation therapy	CMS@GOx	1064	0.48 W cm^{-2}	U14	A multifunctional cascade bioreactor based on hollow mesoporous CMS loaded with glucose oxidase (GOx) enables GOx-catalysis-enhanced PDT/PTT/ICD	166
	CSCs@PEG	1064	0.8 W cm^{-2}	4T1	CSCs@PEG enable a GOx-like activity that consumes glucose, leading to increased H_2O_2 levels, and subsequently more ROS	167
	SC NSs	1064	0.8 W cm^{-2}	4T1	GOx-functionalized nanocatalysts enable cycle-enhanced combination therapy	168
PDT combined with gas therapy	CDs-NO	1064	0.8 W cm^{-2}	4T1	The ROS generated by PDT could rapidly form highly toxic $ONOO^-$ radicals and can also activate an immune response to inhibit tumor metastasis	169
	TiO_2@UCN/Qr/LA	1060	0.6 W cm^{-2}	Saos-2	Phototherapy platform composed of rare-earth elements promotes angiogenesis and inhibits bone tumor growth	110

electronic field and band bending for the balance of Fermi level. When excited by NIR-II light, FeS_2 with lower band gap (1.16 eV) is excited first. At the same time, the thermal energy ($E_{thermal}$) of the nanocomposite is enhanced due to the photothermal effect. When the sum of $E_{thermal}$ and E_{light} is greater than the bandgap of CoS_2 (1.37 eV), photogenerated charges are excited, and the electrons in the conduction band of FeS_2 tend to migrate to the valence band of CoS_2, accomplishing the combined effect of PDT and PTT (Fig. 10b and c). Xu *et al.*[123] ingeniously designed MoO_3-starring silica nanozymes (HMMSNs@HA), which can accomplish NIR-II light-triggered photonic thermal-enhanced ROS production. In this context, the regulation of hydrogenation induces intervalence charge transfer among Mo^{4+}, Mo^{5+}, and Mo^{6+}, which triggers an induced LSPR effect in HMMSNs@HA, enhancing its photothermal conversion capabilities. Consequently, the increased presence of lower-valence Mo facilitates the conversion of H_2O_2 to •OH. Moreover, it is well-known that tumor environments frequently lack oxygen (are hypoxic) and cannot supply adequate oxygen to enhance rates of reactive oxygen species (ROS) production. In response to hypoxia in solid tumors, various plasmon-pyroelectric nanostructures were developed by Zhang's group[180–182] to produce a temperature-mediated ROS, which represents an ingenious way to combine PTT with PDT. These studies showed that under repeated thermal excitation, pyroelectric materials can efficiently convert thermal energy into electrical energy, thereby facilitating the sustained separation of electrons and holes, showing great potential for ROS generation.

PDT is an efficient strategy to circumvent the thermotolerance of tumor cells and thus boost the efficacy of PTT. ROS generated by PDT can oxidize proteins,[183] including HSPs, resulting in damage to tumors.[184] Bu *et al.*[178] employed SnSe-polyvinylpyrrolidone (SnSe-PVP) nanorods, a pyroelectric biomaterial with potent ROS-generating abilities, to facilitate the conversion of temperature fluctuations into pyroelectric

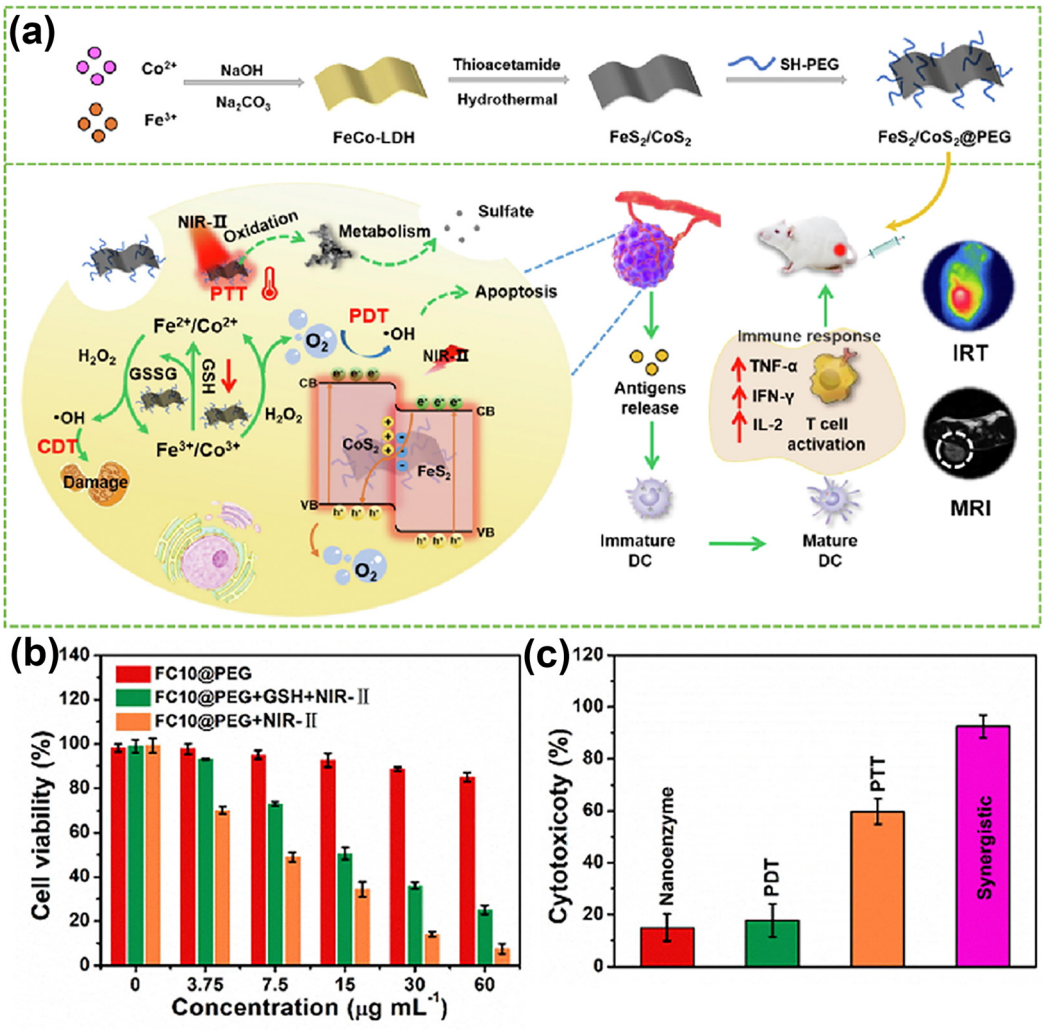

Fig. 10 (a) Schematic illustration of therapeutic effects of FC10@PEG NSs. (b) MTT assay of HepG-2 cells co-cultured with FC10@PEG with/without NIR irradiation. (c) Cytotoxicity induced from CDT, PDT, PTT, and synergistic PDT/PTT/CDT. Reproduced with permission from ref. 156. Copyright 2014, Elsevier.

charges during heating and cooling phases. These charges can then interact with surrounding oxygen molecules to produce ROS, counteracting the adverse effects of HSPs. This approach effectively lowers the thermoresistance of tumor cells, thereby enhancing the PTT efficacy. Wang *et al.*[181] developed a high-performance pyroelectric nanocatalyst, $Bi_{13}S_{18}I_2$ nanorods, to overcome the intrinsic drawbacks of conventional PTT. They demonstrated that by subjecting cells to alternating cooling and heating, ROS can eradicate the molecular chaperone heat shock protein 90 (HSP90), enhancing the effectiveness of photothermal hyperthermia through the transfer of charges generated by pyroelectricity. This approach achieved a tumor inhibition rate of 97.2%.

4.2. Combining photodynamic therapy and chemotherapy

Chemotherapy is extensively employed in the traditional treatment of diverse tumors. However, the administration of chemotherapy introduces the challenge of drug resistance, significantly impacting clinical effectiveness. This issue is particularly pronounced in single-agent chemotherapy regimens, where the susceptibility to drug resistance phenomena is heightened. The advancement of tumors and the unfavorable prognosis resulting from chemotherapy resistance have emerged as significant clinical challenges requiring urgent resolution. The constrained effectiveness of single-agent therapy in treating tumors, coupled with the development of resistance, underscores the imperative need for an integrated treatment model. The combination of PDT with chemotherapy has long been investigated in combating cancer.[35,185,186] Next, we delve into a series of recent studies that have meticulously explored interactions and complementary approaches between chemotherapy and PDT. These investigations highlight that combining chemotherapy and PDT is a promising strategy for effective tumor treatment.

First, it should be stressed on the fact that chemotherapy can be highly efficient in overcoming the drawbacks of PDT, such as low oxygen concentration and limited light penetration, thus enabling complementary treatment of tumors.[187–189] For

example, Sun's team[187] reported a "three birds with one stone" strategy by demonstrating a type of nanoparticles activated by adenosine triphosphate (ATP). Inside tumor cells, these nanoparticles escaped from lysosomes on account of holding a positive charge and were broken down by the high concentration of ATP in the cytoplasm. This process resulted in the release of NIR photosensitizers (Cy-I) and chemotherapeutic agents (DPA-Cd) in the tumor cells, leading to the combined treatment of PDT and chemotherapy to achieve tumor suppression. Qin *et al.*[162] proposed multilayered Fe_2O_3 structures (UF@PPDF NPs), in which hierarchical assemblies of γ-Fe_2O_3 nanocrystals greatly improved the efficiency of iron utilization and achieved extremely high NIR-II photothermal conversion efficiencies, together with highly useful theranostic capabilities based on switchable magnetic resonance imaging. These theranostic probes also possessed outstanding abilities for the controlled release of chemotherapeutic drugs, iron, and ions. These substances could generate the highly toxic radical $^{\bullet}OH$ in acidic environments, offering novel avenues for highly efficient diagnosis and treatment of deep-seated tumors. Additionally, Chen's team[161] developed a nanoplatform coloaded with copper selenide quantum dots ($Cu_{2-x}Se$ QDs) and tirapazamine (TPZ) for precise chemodynamic/photodynamic/hypoxia-activated chemo trimodal synergistic therapy. The presence of oxygen-depleting PDT mediated by $Cu_{2-x}Se$ QDs further exacerbated tumor hypoxia, effectively activating the cytotoxicity of TPZ for tumor eradication.

Furthermore, it is crucial to emphasize that photoactivation can serve not only to harm and sensitize tumors but also to regulate the release of drugs, hinder escape pathways that could lead to drug resistance or cell proliferation, diminish the compensatory activation of survival pathways, and potentially restore sensitivity in drug-resistant cells. Moreover, by employing such strategies, drug resistance can even be reversed.[188,190] In a noteworthy study, Gao's team[150] combined Nb_2C plasmon, Pt nanoenzymes, Doxorubicin (DOX), and tumor cell membranes to form the plasmonic assembly NPD@M (Fig. 11a). The remarkable photothermal characteristics of Nb_2C when exposed to NIR-II light were utilized to expand tumor vessels (Fig. 11b), thereby improving blood perfusion and drug extravasation. Simultaneously, these properties were leveraged to boost the catalytic activity of the nanoenzymes. Moreover, within the tumor microenvironment, doxorubicin (DOX) was released under elevated thermal and

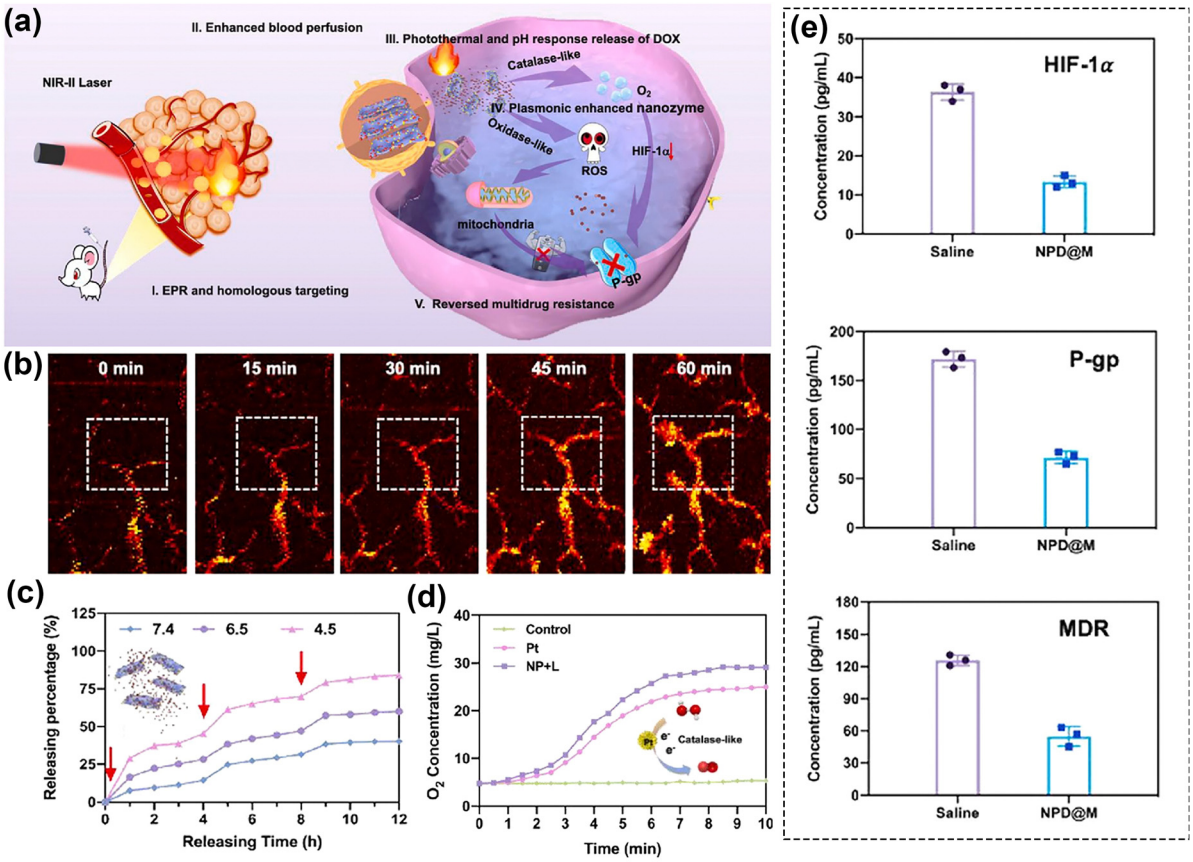

Fig. 11 (a) Schematic diagram of the therapeutic process of NPD@M *in vivo*. (b) Photoacoustic images of tumor blood vessels in the mice treated with NPD@M at different time points. (c) The curves of photothermal and pH-responsive drug release. (d) The generation of dissolved oxygen under different treatments. (e) the concentration of HIF-1α, P-gp and MDR1 of saline and NPD@M + Laser. Reproduced with permission from ref. 150. Copyright 2021, Elsevier.

acidic conditions, facilitating targeted chemotherapy. The NPD@M nanoplatform demonstrated the capability to release up to 80% of the drug after three rounds of laser exposure as shown in Fig. 11c. Taking advantage of the high concentration of H_2O_2 in the tumor microenvironment, more O_2 was generated due to the excellent catalase (CAT) activity of Pt nanoenzymes (Fig. 11d). These were successfully used to alleviate tumor hypoxia and to down-regulate the expression of hypoxia-inducible factor (HIF-1α). At the same time, combined PDT-generated ROS reduced mitochondrial energy supply to P-gp glycoprotein, a membrane efflux pump that recognizes and transports chemotherapeutic agents out of cells. The authors verified the enhancement in blood perfusion volume and the down-regulation of HIF-1α by photoacoustic imaging (Fig. 11b) and ELISA measurements (Fig. 11e), respectively. The integration of this comprehensive approach has been showcased as an excellent tool for overcoming multidrug resistance and enhancing the efficacy of chemotherapy, introducing a novel concept for the utilization of plasmonics in anti-tumor therapy.

4.3. Combining photodynamic therapy and immunotherapy

Cancer immunotherapy involves activating the immune system to combat cancer or bolster its inherent defense mechanisms.[13,191] The evasion of immune surveillance by cancer cells through various pathways, allowing them to elude elimination by the host immune system, is a recognized phenomenon. Consequently, an increasing number of studies are exploring the utilization of photodynamic nanomedicines in conjunction with immune checkpoint inhibitors and adjuvants. Such approaches aim to enhance both direct and systemic therapeutic effects, offering potential avenues for effectively treating heterogeneous tumors.[192] Furthermore, accumulating evidence suggests that PDT has the capability to trigger an anti-tumor immune response, specifically by inducing tumor immunogenic cell death (ICD).[18,193–195] This process ultimately leads to the systemic inhibition of subsequent tumor growth in distant sites and serves as a defense against tumor recurrence.[196] Some examples are as follows: (a) PDT-mediated enhancement of ROS promotes reprogramming of tumor-associated macrophages phenotype, that is, converting cold tumors into hot tumors, thereby promoting intratumoural T cell infiltration.[78] (b) PDT can promote mutations of antigen presenting cells and cytotoxic T lymphocytes to homing.[13] (c) During PDT calreticulin moves from the endoplasmic reticulum to the cell membrane's surface and provides an ''eat me'' signal to cause an immune response.[197] PDT can thus be harnessed for immunotherapy by fostering an anti-tumor immune response within the body.

Past studies showed that, NIR-II PDT has the capability to directly initiate adaptive immune responses.[51] Canti *et al.*[198] found that PDT can trigger anti-tumor immunity, while Liu *et al.*[199] demonstrated the synergistic effect of PDT and immune checkpoint inhibitors *via* the phthalocyanine dye-labeled probe. Later, Lin *et al.*[200] employed a nanoscale metal–organic framework (nMOF) with anti-PD-L1 antibody, which not only converted endogenous H_2O_2 to O_2 for oxygen-dependent PDT, but also improved cancer immunotherapy through infiltration of cytotoxic T cells. Recently, Yang *et al.*[164] reported for the first time a corn-like Au/Ag nanorod (Au/Ag NR) that could reprogram the immunosuppressive cold tumor microenvironment under NIR-II triggering *via* PTT/PDT, synergizing with the immune-checkpoint blockade (ICB) antibody aCTLA4 to achieve enhanced cancer therapy. Fig. 12a–c show the synergistic effect of the Au/Ag NR with the ICB antibody. In contrast, the heat and ROS generated by the Au/Ag NR upon 1064 nm light irradiation further triggered the ICD of tumor cells, activated the antibody, and effectively delayed secondary tumor growth (Fig. 12b). As shown in the Fig. 12d, by combining the PDT treatment with ICB antibody, the conversion of cold tumor to hot tumor was achieved. This transformation provided protection to the mice used as animal model from tumor cell re-attack even 40 days post-treatment. The approach significantly elevated the infiltration of T-cells into the tumor, thereby initiating a systemic immune response and effectively delaying the growth of 4T1 tumors in the mice. This approach was demonstrated thus as a highly useful solution to augment the infiltration of T-cells within the tumor, activating a robust systemic immune response. This improved method exhibited heightened efficacy in preventing the recurrence of 4T1 tumors in the considered murine tissues, effectively hindering the growth of distant tumors.

In addition to inhibiting primary tumor growth, previous studies have showed that PDT-induced immunogenic cell death can prevent metastasis;[197] this was demonstrated on lung tissue. An *et al.*[165] proposed a NIR-II laser-mediated photo-Fenton-like reaction based on a plasmonic self-doped semiconductor Cu_8S_9. Under mild NIR-II laser irradiation ($0.2\ W\ cm^{-2}$), Cu_8S_9 experienced Cu(II)/Cu(I) valence conversion according to the mechanism of plasmon-induced electron transfer, resulting in high generation of $^{\bullet}OH$, which directly induced ICD, release of death-associated molecular patterns (DAMPs), and maturation of daughter cells (DCs) in tumor cells. The efficacy of the immunotherapy induced by the enhanced ROS was investigated using changes in DAMPs, including the translocation of calreticulin (CRT) on the cell membrane surface, the extracellular release of adenosine triphosphate (ATP), and high mobility group box-1 protein (HMGB1). Additionally, the authors further evaluated DCs maturation by measuring the ratio of mature DCs ($CD11c^+CD80^+CD86^+$). The Cu_8S_9 + laser group was approximately 1.5-time higher than Cu_8S_9 alone, indicating that the NIR-II laser-mediated enhanced ROS could induce more mature DCs. Jiang *et al.*[108] similarly constructed a plasmonic gold nanobipyramid@cuprous oxide (Au NBP@Cu_2O)-mediated promising strategy to tackle metastatic tumors. When comparing metastasis in the liver and lungs, PDT mediated by Au NBP@Cu_2O helped maintain the intact structures of both organs.

4.4. Combining photodynamic therapy and starvation therapy

Tumor starvation therapy aims to impede the growth and reproduction of tumor cells by cutting off the energy supply,

which means interfering with tumor angiogenesis, consumption of glucose by glucose oxidase (GOx) and inhibiting the function of glucose transporter proteins on the surface of tumor cell membranes.[201] This significantly hinders the growth and reproduction of tumors, and contributes to their erradication.[166,202–205] In general, due to the Warburg effect, the concentration of glucose in tumor cells is higher than in normal cells.[206–208] Loading GOx in nanomaterials can ensure properties of the material as well as deplete intracellular glucose through a glucose-related reaction that catalyzes the conversion of glucose to gluconic acid and H_2O_2. This process not only depletes intracellular glucose for starvation therapy, but also increases endogenous levels of H_2O_2 to generate ROS for PDT.[208] Thus, GOx has been widely employed to construct multifunctional nanoplatforms to enable PDT in combination with starvation therapy or cascade reactions for the purpose of enhancing the efficacy of PDT.[166,205] Zhang *et al.*[127] developed nanoassemblies comprising copper surface-modified oxygen-deficient titanium dioxide (TiO_{2-x}) and sulfur-doped mesoporous organosilica, onto which GOx was loaded (TiO_{2-x}@Cu,S-MONs@GOx). The GOx could catalyze the redox reaction of glucose, which in turn resulted in a large amount of H_2O_2 for PDT. This cascade reaction resulted in a reduction of cell survival from 83% (TiO_{2-x}@Cu,S-MONs-treated group) to less than 20%. Another study by Lin *et al.*[166] employed hollow mesoporous Cu_2MoS_4 bioreactors loaded with GOx, and the bioreactors showed similar outcomes.

In another study, Lin *et al.*[209] argued that the use of natural enzymes inherently suffers from high costs and susceptibility to inactivation. Consequently, they synthesized a di-shell hollow

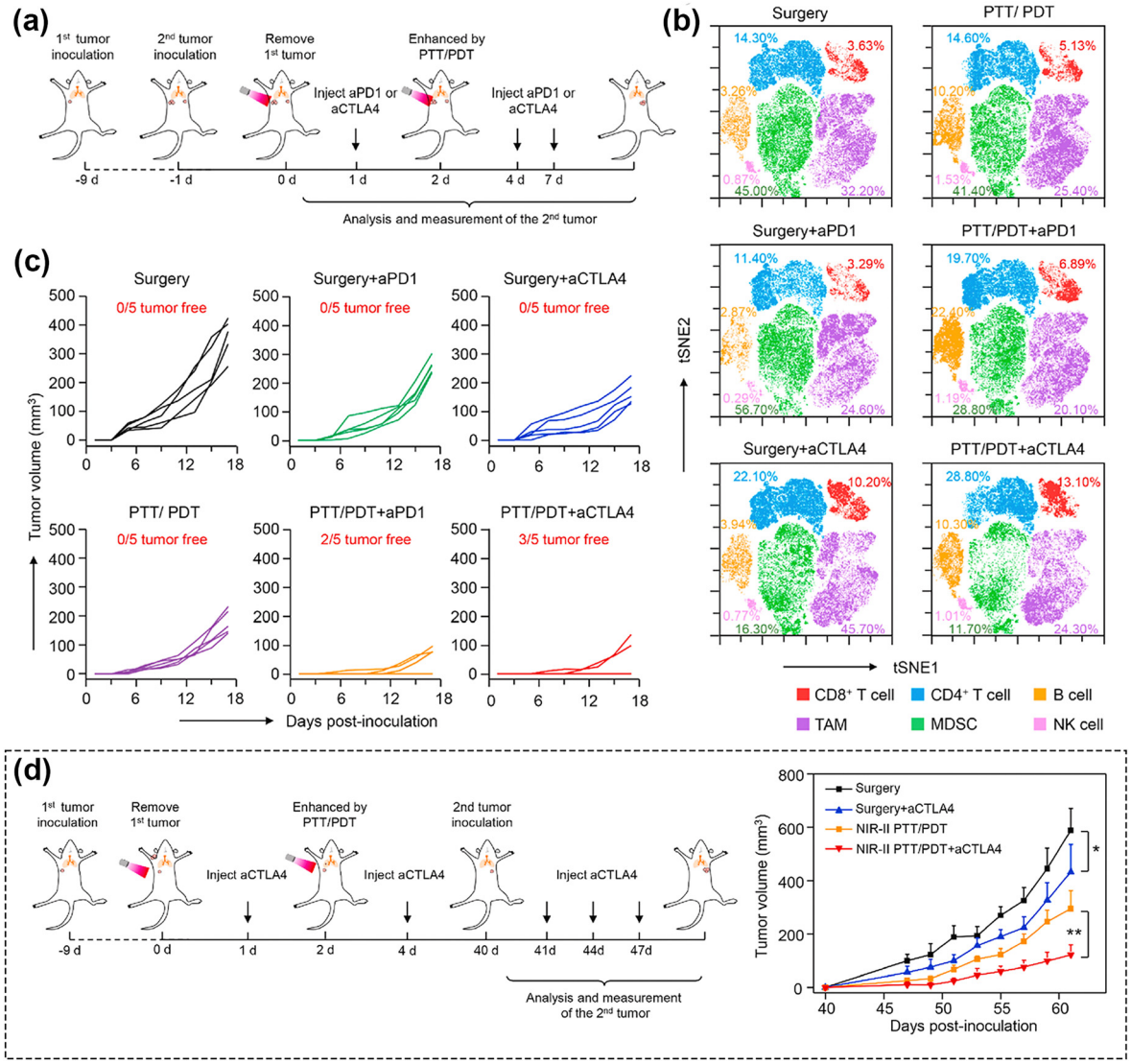

Fig. 12 (a) Schematic illustration showing the combination of Au/Ag NR-mediated NIR-II PTT/PDT and ICB antibodies. (b) Individual tumor growth curves of distant tumors of mice treated to generate a secondary tumor. (c) t-SNE analysis of immune cells in tumors from mice at the end of therapy. (d) Schematic illustration showing the combination of Au/Ag NRs-mediated NIR-II PTT/PDT and ICB antibodies to inhibit rechallenged tumors. (e) Tumor growth curves of rechallenged tumors. Reproduced with permission from ref. 164. Copyright 2021, Elsevier.

nanoheterostructure of Mn-doped CoS@carbon (CMS/C), aiming to develop a high-performance nanoenzyme and photosensitizer for anticancer applications. Co^{2+}/Mn^{2+} ions catalyzed H_2O_2 to generate $^{\bullet}OH$ and Co^{3+}/Mn^{3+} ions, which in turn reacted with H_2O_2 to generate O_2 and Co^{2+}/Mn^{2+}, exhibiting POD- and CAT-like activities, respectively. Following this line of investigation, they constructed Co_9S_8/S-CDs@PEG (CSCs@PEG) nanoheterostructures instead of using approaches based on GOx loading to achieve glucose consumption to inhibit tumor growth.[167] These nanocomposites enabled not only the simultaneous excitation of PTT and PDT, but also the reduction of intracellular energy supply and the increase of H_2O_2 content through GOx-like properties. The consumption of glucose demonstrated *via* a series of experiments including the UV-visible absorption spectra of TMB and $KMnO_4$ solution, or assessment of changes in pH and cyclic voltammograms of the CSCs@PEG solution with or without the addition of glucose. However, the catalytic activity of nanozymes with single-enzyme mimetic activity is restricted by TME. For example, the insufficient supply of H_2O_2 always reduces the therapeutic efficacy of POD-mimicking nanozymes.[210] In such a scenario, the construction of multifunctional nanoplatforms by high-efficiency nanozymes with multi-enzyme mimetic activities to ensure the massive production of ROS is of great significance. Zhu's group[59] constructed a novel mild hyperthermia-enhanced nanocatalytic therapy platform with triple enzyme-mimic activities (CD@Nb_2C). The enzyme-like activities of POD, CAT, and GPX were assessed in a mild temperature (43 °C) and acid environment (Fig. 13a). The 3,3′,5,5′-tetramethylbenzidine absorbance of CD@Nb_2C increased significantly upon increasing the H_2O_2 concentration, acidity, and temperature (Fig. 13b–d), demonstrating that the mild photothermal treatment facilitated the POD-mimic activity. Similar results were observed by electron spin resonance (ESR) spectroscopy (Fig. 13e). In addition to POD-mimicking catalytic activity, CAT-mimicking activity and GSH depletion capacity of CD@Nb_2C nanoenzymes were assessed by changes in the peak 5,5-dithiobis (2-nitrobenzoic acid) uptake and the production of dissolved oxygen, respectively (Fig. 13f and g). Interestingly, the presence of CD@Nb_2C heterojunction accelerated electron transfer processes and enhanced the catalytic activity of CD@Nb_2C for improving the ROS generation (Fig. 13h). Nanoenzymes as an indirect strategy to enhance the therapeutic efficacy of ROS-based PDT have been identified as a promising future trend for the cancer treatment.[211]

4.5. Combining photodynamic therapy and gas therapy

Gas mediators play a pivotal role *in vivo* by exerting diverse biological functions within both tumor cells and host tissues, as highlighted in many studies.[212–215] Among these, H_2, CO_2, NO, H_2S and SO_2 are extensively acknowledged as gaseous signaling molecules that participate in the transmission of signaling pathways.[215,216] Delivery of exogenous gases aims to induce depolarization of the mitochondrial membrane potential, which further damages the mitochondria and leads to the release of mitochondrial DNA into the cytoplasm.[214] Utilizing gas therapy represents an innovative approach to enhance synergistic treatment in conjunction with other cancer therapies. Interestingly, NO has different effects on various physiological processes depending on the concentration. Whereas low concentrations of NO promote cancer growth attributed to enhanced angiogenesis and metastasis, higher levels of NO inhibit cancer progression by inducing apoptosis, sensitizing tumors to therapeutic treatments, reversing drug resistance, and delaying metastasis.[169,217,218] Zhang *et al.*[219] put forward an "O_2-economizer" agent for PDT of hypoxia tumors according to the principle of cellular respiration inhibition by NO, while Ge *et al.*[220] improved the wavelength range of the excitation light source and designed a combined PTT/PDT/NO nanoplatform. It promoted the release of ROS and NO through the warming effect, whereas the release of ROS and NO in turn enhanced the photothermal killing effect.

Along with increasing the sensitivity of cancer cells to ROS, NO binds with ROS to produce peroxynitrite anions ($ONOO^-$), which can damage the DNA of tumor cells. Under active conditions, $ONOO^-$ can also produce strong oxidants such as $^{\bullet}OH$ and NO_2 radicals through cleavage and interaction with CO_2. L-Arginine (L-Arg) is an endogenous NO donor with good biosafety, and it has been demonstrated by the groups of Cai[221] and Liu[222] that photosensitizers with L-Arg decoration can be used to achieve cascade-amplified therapeutic effects. However, the approach of combining NO donors with photosensitizers typically involves intricate assembly, often including elements that don't directly contribute to anticancer effects. Lin's group[169] developed nanoparticles called C–NO, which exhibit GSH-sensitive nitric oxide (NO) release and *in situ* conversion of nitrated cyclodextrins (CDs) (Fig. 14a). In the presence of GSH, the nitrated CDs were shown to be able to release NO, meaning that the designed and fabricated nanomaterials have the ability of tumor-targeted NO release (Fig. 14b). On these grounds, the *in situ* generation of ROS under NIR-II irradiation can capture NO to form $ONOO^-$,[223] which improves the cytotoxicity and accelerates the half-life. The authors demonstrated the successful construction of a GSH-sensitive NO-releasing nanoplatform through a series of experiments. Specifically, ESR spectra showed significant NO radical signals (Fig. 14c). Intracellular green fluorescence confirmed that NO production was triggered from endogenous GSH (Fig. 14e). Importantly, validation experiments on GSH depletion illustrated from another angle that there was no NO release without GSH (Fig. 14d). This strategy of *in situ* conversion solves the problem of short half-life of NO and improves the efficiency of $ONOO^-$ formation. Besides NO, there are other gas molecules that play important roles in anticancer therapies, such as H_2S. Considerable focus has been directed towards the on-site generation or release of surplus H_2S to enhance tumor suppression by combination therapies.[214] Moreover, a growing number of efforts are devoted to exploring the prospect that H_2S has the potential to reshape TME and stimulate robust anti-tumor immunity within the organism.[224] The swift progress on fundamental research associated with gas therapy has led to the initiation of numerous clinical trials for treating diverse inflammatory

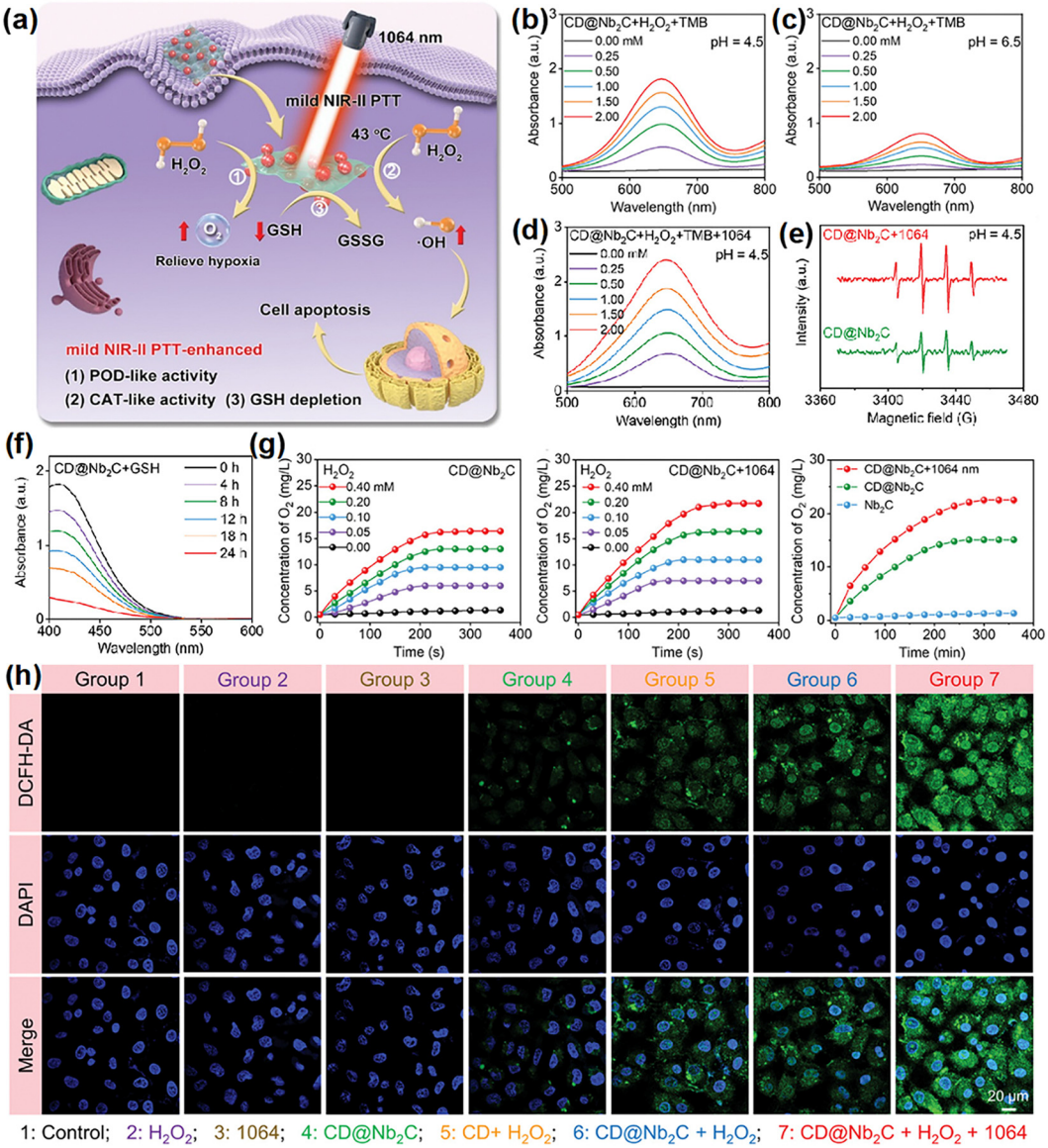

Fig. 13 (a) A schematic illustration of the catalytic pathways of CD@Nb_2C nanozymes with POD-, CAT-, and GPX-mimic activities. (b)–(d) Absorption spectra of the oxidized 3,3′,5,5′-tetramethylbenzidine catalyzed by CD@Nb_2C nanozymes at varied pH or under mild NIR-II laser irradiation. (e) ESR spectra indicating •OH generated by CD@Nb_2C nanozymes. (f) The GSH depletion activity evaluation of CD@Nb_2C nanozymes. (g) O_2 generation under different treatments. (h) ROS staining of 4T1 cells after treated. Reproduced with permission from ref. 59. Copyright 2023, Wiley.

cancer-related conditions. This underscores the need for further exploration of nanoplatforms combining gas therapy with PDT.[212]

5. Conclusions and perspectives

In recent decades, the application of PDT has been observed in diverse clinical treatments for various diseases. However, a longstanding challenge in PDT remains the effective delivery of light, particularly in the treatment of deep-seated tumors. In the present era, photosensitizers activated by near-infrared-II (NIR-II) light exhibit reduced tissue autofluorescence, enhanced spatial resolution, and a higher signal-to-background ratio. These improvements are attributed to the diminished absorption of NIR-II light and reduced photon scattering. In this review, we discussed the fundamental principles of PDT and provided an overview of diverse types of photosensitizers activated by NIR-II light. Additionally, we encompassed the advancements in diverse multi-term synergistic therapies developed in the field of oncology, building on PDT in association with complementary therapeutic strategies.

Despite the promising aspects of NIR-II-activated PDT, certain considerations warrant further attention in future research for the design and construction of PDT schemes (Fig. 15). Primarily, the issue of nanomaterial retention in normal tissues and organs, particularly in the liver, poses a significant concern. Additional work to resolve such issues could ultimately lead to reduced accumulation in tumors by ensuring the rapid

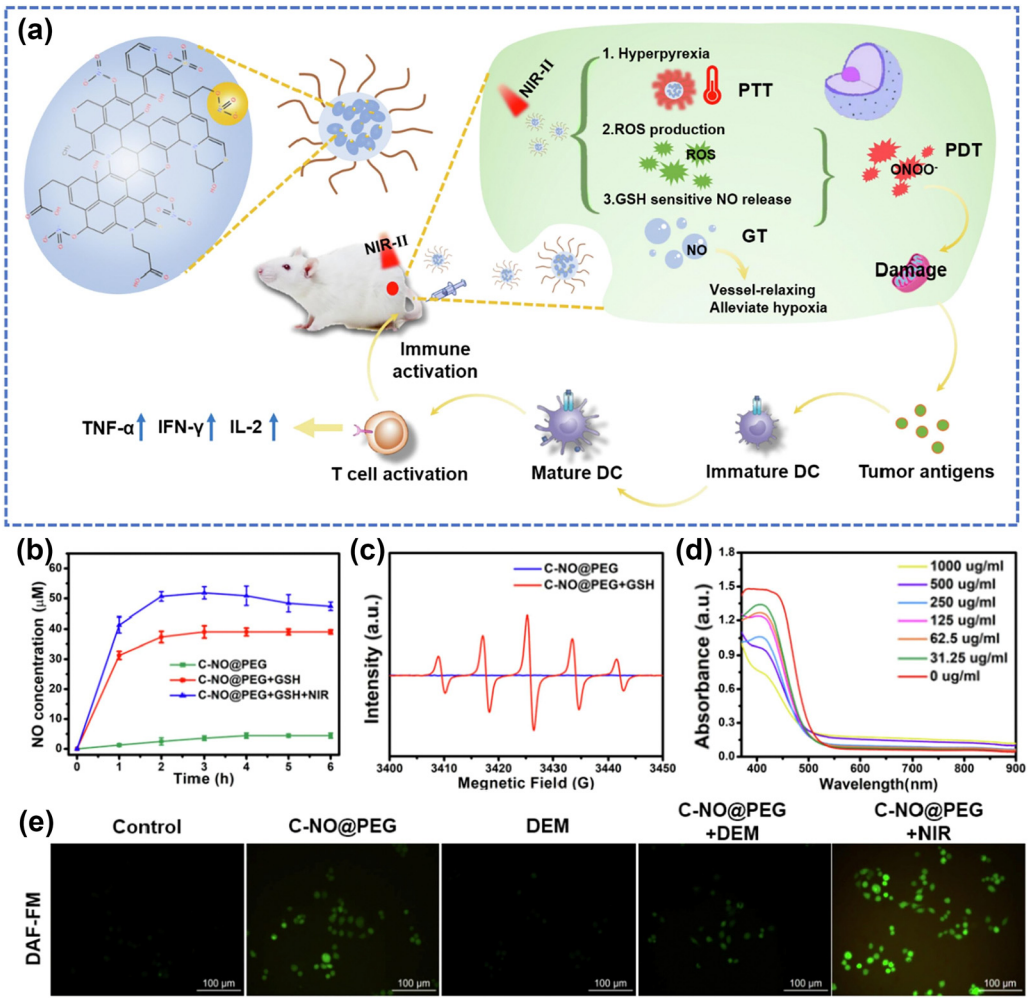

Fig. 14 (a) Schematic illustration of C–NO nanocomposites for synergistic NO therapy and phototherapy. (b) NO release from C-NO treated with different conditions. (c) ESR spectra of PTIO under different treatments. (d) The depletion of GSH at different concentrations of C-NO@PEG. (e) The fluorescence imaging of 4T1 cells treated by C-NO@PEG (DAF-FM was acted as a typical NO probe). Reproduced with permission from ref. 169. Copyright 2022, Elsevier.

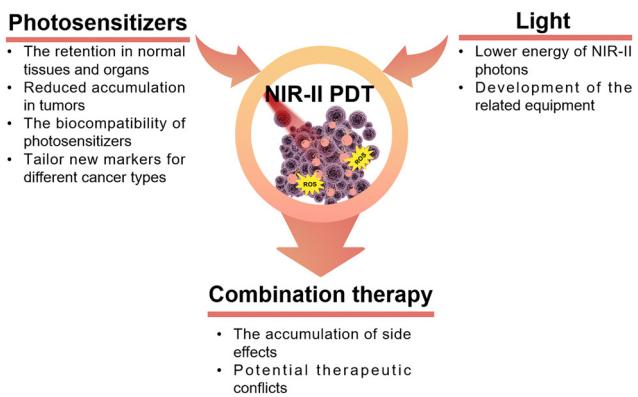

Fig. 15 Typical ongoing challenges for enhancing the therapeutic effectiveness of NIR-II PDT.

circulation of nanomaterials in the bloodstream. However, there are still many subtle aspects associated to this process that have not been fully elucidated, but recent progress in label-free *in vivo* tissue imaging[225,226] promises swift progress in this area, especially with the recent advent of user-friendly super-resolved methods for non-linear optical imaging.[227,228] Regarding tumor-targeted nanomaterials, uncertainties still persist on their targeting capabilities and therapeutic efficacy due to the variability of the TME. Numerous studies have employed universal markers for cancer, such as the receptor CD44,[229] integrin αvβ3,[230] and there is an urgent need to develop new strategies to tailor new markers for different cancer types and cancer cell subtypes, such as genes[231–233] and blood vessels,[234] to achieve better specificity in the cancer cell killing process. Secondly, most NIR-II photosensitizers currently rely on excitation at 1064 nm, overlooking other wavelength-excited photosensitizers. In other words, NIR-II-triggered PDT is still in its early stages. The advancement of alternative NIR-II-activated photosensitizers necessitates collaborative efforts across interdisciplinary fields, including chemistry, materials science, pharmaceutics, and medicine. Additionally, the development of photosensitizers with high light conversion efficiency is

crucial to address the challenge of less efficient generation of ROS due to the lower energy of NIR-II photons. Thirdly, many existing studies on the biocompatibility of nanomaterials are inadequate, lacking crucial aspects such as biodistribution *in vivo* and pharmacokinetics. This deficiency presents a bottleneck in the clinical translation of these materials. Hence, there is a pressing need for additional research focusing on factors like uptake, circulation, retention, degradation, and elimination to pave the way for the clinical application of nanomaterial-based PDT in cancer treatment. Moreover, the design and development of NIR-II photosensitizers should take into account their potential for multimodal therapeutic diagnostics. Both inorganic and organic nanomaterials have the capability to serve as carriers for additional active ingredients with diverse therapeutic mechanisms. For example, mesoporous materials can be loaded with chemotherapeutic drugs, serving as effective tools to regulate the targeted release of drugs through the TME. Under NIR light irradiation, these materials can synergistically generate ROS, ultimately facilitating the construction of combined chemotherapy/PDT nanoplatforms.[159] Along with the rapid advancements of NIR-II fluorescent or photoacoustic probes, it is possible to achieve fluorescence/photoacoustic imaging and PDT simultaneously, which allows precise control of PDT spatio-temporally and spatio-temporally.[53]

As emphasized in this review, numerous approaches that combine complementary therapies offer promising prospects for tumor treatment. Nevertheless, there is no single combination therapy that addresses all involved aspects and meets all the needs of tumor treatment at the same time. The concept of "1 + 1 > 2," often mentioned in various articles, not only indicates the synergistic effects between multiple treatment modalities but may also imply the potential accumulation of side effects. Further exploration is required to understand how to mitigate potential therapeutic conflicts when combining complementary therapies.

We aspire that this review will catalyze future advancements in enhancing the therapeutic effectiveness of PDT for deep-seated tumors and contribute to a more profound understanding of the existing gaps in PDT research.

Author contributions

Y. Yang: information collection, visualization, writing (original draft). Prof. S. Jiang: data curation, formal analysis, visualization. Prof. S. G. Stanciu: validation, funding acquisition, project administration, writing (review and editing). Dr H. Peng: methodology, data curation, visualization, writing (review and editing). Prof. A. Wu: conceptualization, resources, supervision, writing (review and editing). Dr F. Yang: conceptualization, project administration, supervision, funding acquisition, writing (original draft and editing).

Data availability

No primary research results, software or code have been included and no new data were generated or analysed as part of this review.

Conflicts of interest

There are no conflicts to declare.

Acknowledgements

FY acknowledges the support of the National Key R&D Program of China (No. 2022YFF1202000, Subproject No. 2022YFF1202003), the Youth Innovation Promotion Association, Chinese Academy of Sciences (2022301), Ningbo 3315 Innovative Talent Project (2018-05-G), "Innovation Yongjiang 2035" Key R&D Programme of Ningbo (2024Z217) and Special Exchange Program of Chinese Academy of Sciences (China-Romania). SGS acknowledges the support of UEFISCDI Grant RO-NO-2019-0601 MEDYCONAI. SGS and FY express sincere thanks to the COST ACTION 19118 ESSENCE for facilitating fruitful discussions, and idea exchange.

References

1 Y. Yang, P. Wang, R. Shi, Z. Zhao, A. Xie, Y. Shen and M. Zhu, *Chem. Eng. J.*, 2022, **441**, 136042.
2 N. G. Zaorsky, T. M. Churilla, B. L. Egleston, S. G. Fisher, J. A. Ridge, E. M. Horwitz and J. E. Meyer, *Ann. Oncol.*, 2017, **28**, 400–407.
3 W. Chen, R. Zheng, S. Zhang, H. Zeng, C. Xia, T. Zuo, Z. Yang, X. Zou and J. He, *Cancer Lett.*, 2017, **401**, 63–71.
4 J. Qi, M. Li, L. Wang, Y. Hu, W. Liu, Z. Long, Z. Zhou, P. Yin and M. Zhou, *Lancet Public Health*, 2023, **8**, e943–e955.
5 E. Kamya, Z. Lu, Y. Cao and R. Pei, *J. Mater. Chem. B*, 2022, **10**, 9770–9788.
6 Z. He, H. Su, Y. Shen, W. Shi, X. Liu, Y. Liu, F. Zhang, Y. Zhang, Y. Sun and D. Ge, *RSC Adv.*, 2019, **9**, 9968–9982.
7 H. H. Lv, Y. C. Zhu, J. P. Xue, X. Jia and J. J. Chen, *Langmuir*, 2022, **38**, 15766–15775.
8 X. Liang, M. Chen, P. Bhattarai, S. Hameed, Y. Tang and Z. Dai, *ACS Nano*, 2021, **15**, 20164–20180.
9 W. Tao, N. Wang, J. Ruan, X. Cheng, L. Fan, P. Zhang, C. Lu, Y. Hu, C. Che, D. Sun, J. Duan and M. Zhao, *ACS Appl. Mater. Interfaces*, 2022, **14**, 6404–6416.
10 H. Hou, X. Huang, G. Wei, F. Xu, Y. Wang and S. Zhou, *ACS Appl. Mater. Interfaces*, 2019, **11**, 29579–29592.
11 M. Ethirajan, Y. Chen, P. Joshi and R. K. Pandey, *Chem. Soc. Rev.*, 2011, **40**, 340–362.
12 J. Xie, Y. Wang, W. Choi, P. Jangili, Y. Ge, Y. Xu, J. Kang, L. Liu, B. Zhang, Z. Xie, J. He, N. Xie, G. Nie, H. Zhang and J. S. Kim, *Chem. Soc. Rev.*, 2021, **50**, 9152–9201.
13 B. Ji, M. Wei and B. Yang, *Theranostics*, 2022, **12**, 434–458.
14 X. L. Li, C. Jiang, X. L. Jia, Y. Y. Cao, Y. Q. Mao, J. N. Hao, Y. Yang, P. Zhang and Y. S. Li, *Adv. Healthcare Mater.*, 2023, **12**, 2202467.
15 Z. J. Zhou, J. B. Song, L. M. Nie and X. Y. Chen, *Chem. Soc. Rev.*, 2016, **45**, 6597–6626.
16 C. S. Wu, M. H. Cui, L. Cai, C. Chen, X. H. Zhu, Y. H. Wu, J. L. Liu, H. J. Wang and Y. Zhang, *ACS Appl. Mater. Interfaces*, 2022, **14**, 13094–13106.

17 Q. Q. Xiang, C. Yang, Y. L. Luo, F. Liu, J. Zheng, W. W. Liu, H. T. Ran, Y. Sun, J. L. Ren and Z. G. Wang, *Small*, 2022, **18**, 2107809.
18 K. Xiong, F. M. Wei, Y. Chen, L. N. Ji and H. Chao, *Small Methods*, 2022, **7**, 2201403.
19 Z. Wang, F. Zhang, D. Shao, Z. Chang, L. Wang, H. Hu, X. Zheng, X. Li, F. Chen, Z. Tu, M. Li, W. Sun, L. Chen and W. F. Dong, *Adv. Sci.*, 2019, **6**, 1901690.
20 W. Li, J. Yang, L. Luo, M. Jiang, B. Qin, H. Yin, C. Zhu, X. Yuan, J. Zhang, Z. Luo, Y. Du, Q. Li, Y. Lou, Y. Qiu and J. You, *Nat. Commun.*, 2019, **10**, 3349.
21 Y. Su, X. Zhang, Y. Wei, Y. Gu, H. Xu, Z. Liao, L. Zhao, J. Du, Y. Hu, X. Lian, W. Chen, Y. Deng and D. Huang, *ACS Appl. Mater. Interfaces*, 2023, **15**, 6354–6370.
22 P. Jia, Y. Zou and J. Jiang, *ACS Appl. Mater. Interfaces*, 2023, **15**, 22929–22943.
23 X. Tang, X. Chen, S. Zhang, X. Gu, R. Wu, T. Huang, Z. Zhou, C. Sun, J. Ling, M. Liu and Y. Yang, *Adv. Funct. Mater.*, 2021, **31**, 2101320.
24 Y. Jin, Y. Guo, J. Yang, X. Chu, X. Huang, Q. Wang, Y. Zeng, L. Su, S. Lu, C. Wang, J. Yang, J. Qu, Y. Yang and B. Wang, *Adv. Mater.*, 2023, **35**, 2209690.
25 M. Shanmugam, N. Kuthala, R. Vankayala, C.-S. Chiang, X. Kong and K. C. Hwang, *ACS Nano*, 2021, **15**, 14404–14418.
26 E. C. Cheung and K. H. Vousden, *Nat. Rev. Cancer*, 2022, **22**, 280–297.
27 H. Dai, X. Wang, J. Shao, W. Wang, X. Mou and X. Dong, *Small*, 2021, **17**, 2102646.
28 E. Y. Xue, C. Yang, W. P. Fong and D. K. P. Ng, *ACS Appl. Mater. Interfaces*, 2022, **14**, 14903–14915.
29 D. Cui, J. Li, X. Zhao, K. Pu and R. Zhang, *Adv. Mater.*, 2020, **32**, 1906314.
30 S. Zhang, Z. Li, Q. Wang, Q. Liu, W. Yuan, W. Feng and F. Li, *Adv. Mater.*, 2022, **34**, 2201978.
31 Y. Yang, M. Chen, B. Wang, P. Wang, Y. Liu, Y. Zhao, K. Li, G. Song, X. B. Zhang and W. Tan, *Angew. Chem., Int. Ed.*, 2019, **58**, 15069–15075.
32 G. Lan, K. Ni, Z. Xu, S. S. Veroneau, Y. Song and W. Lin, *J. Am. Chem. Soc.*, 2018, **140**, 5670–5673.
33 L. Ding, Y. N. Wu, M. Wu, Q. F. Zhao, H. S. Li, J. F. Liu, X. L. Liu, X. L. Zhang and Y. Y. Zeng, *ACS Appl. Mater. Interfaces*, 2021, **13**, 52435–52449.
34 Y. Jiang, X. Zhao, J. Huang, J. Li, P. K. Upputuri, H. Sun, X. Han, M. Pramanik, Y. Miao, H. Duan, K. Pu and R. Zhang, *Nat. Commun.*, 2020, **11**, 1857.
35 J. C. Li, S. Q. Wang, F. Fontana, C. Tapeinos, M. A. Shahbazi, H. J. Han and H. A. Santos, *Bioact. Mater.*, 2023, **23**, 471–507.
36 B. Sun, J. N. Bte Rahmat and Y. Zhang, *Biomaterials*, 2022, **291**, 121875.
37 T. Shi, C. Huang, Y. Li, F. Huang and S. Yin, *Biomaterials*, 2022, **285**, 121535.
38 S. S. Lucky, K. C. Soo and Y. Zhang, *Chem. Rev.*, 2015, **115**, 1990–2042.
39 X. Z. Zhao, J. P. Liu, J. L. Fan, H. Chao and X. J. Peng, *Chem. Soc. Rev.*, 2021, **50**, 4185–4219.
40 K. Han, Z. Ma and H. Han, *J. Mater. Chem. B*, 2018, **6**, 25–38.
41 Q. Chen, X. Ma, L. Xie, W. Chen, Z. Xu, E. Song, X. Zhu and Y. Song, *Nanoscale*, 2021, **13**, 4855–4870.
42 J. Liu, M. Huang, X. Zhang, Z. Hua, Z. Feng, Y. Dong, T. Sun, X. Sun and C. Chen, *Coord. Chem. Rev.*, 2022, **472**, 214785.
43 X. Xiao, Y. Wang, J. Chen, P. Qin, P. Chen, D. Zhou and Y. Pan, *Biomaterials*, 2022, **289**, 121793.
44 C. Zhang, L. Xu, B. Nan, C. Lu, H. Liu, L. Lei, R. Yue, G. Guan, M. He, X. B. Zhang and G. Song, *ACS Nano*, 2023, **17**, 9529–9542.
45 C. Zhang, X. Hu, L. Jin, L. Lin, H. Lin, Z. Yang and W. Huang, *Adv. Healthcare Mater.*, 2023, **12**, 2300530.
46 G. L. Semenza, *Nat. Rev. Cancer*, 2003, **3**, 721–732.
47 Q. Wang, T. Yang, S. Li, C. Xu, C. Wang, Y. Xiong, X. Wang, J. Wan, X. Yang and Z. Li, *Research*, 2023, **6**, 0223.
48 J. F. Kelly and M. E. Snell, *J. Urol.*, 1976, **115**, 150–151.
49 K. X. Wang, Y. J. Xu, Z. J. Chen, H. X. Li, R. Hu, J. L. Qu, Y. Lu and L. W. Liu, *Nanophotonics*, 2022, **11**, 5089–5100.
50 Z. Y. He, Y. T. Gao, H. M. Zhang, Y. Xue, F. L. Meng and L. Luo, *Adv. Healthcare Mater.*, 2021, **10**, 2101056.
51 Y. Chen, P. Liu, C. Zhou, T. Zhang, T. Zhou, D. Men, G. Jiang and L. Hang, *Acta Biomater.*, 2023, **158**, 649–659.
52 Y. Zhang, Y. Li, J. Y. Li, F. Mu, J. Wang, C. Shen, H. Wang, F. Huang, B. Chen, Z. M. Luo and L. H. Wang, *Adv. Healthcare Mater.*, 2023, **12**, 2300267.
53 C. Y. Cao, H. Zou, N. Yang, H. Li, Y. Cai, X. J. Song, J. J. Shao, P. Chen, X. Z. Mou, W. J. Wang and X. C. Dong, *Adv. Mater.*, 2021, **33**, 2106996.
54 X. J. Li, B. Li, W. B. Zhang, Z. M. Chen, J. P. Liu, Y. Shi, H. Y. Xu, L. W. Shan, X. Liu and L. M. Dong, *Dalton Trans.*, 2023, **52**, 11458–11464.
55 F. Wu, H. Chen, Q. Li, R. Liu, Y. Suo, B. Li, X. Kong, Z. Cheng, H. Liu and Y. Chang, *Chem. Eng. J.*, 2023, **468**, 143827.
56 S. Bi, Z. Deng, J. Huang, X. Wen and S. Zeng, *Adv. Mater.*, 2023, **35**, 2207038.
57 Q. Cai, C. Wang, S. L. Gai and P. A. P. Yang, *ACS Appl. Mater. Interfaces*, 2022, **14**, 3809–3824.
58 K. Y. Pham, L. C. Wang, C. C. Hsieh, Y. P. Hsu, L. C. Chang, W. P. Su, Y. H. Chien and C. S. Yeh, *J. Mater. Chem. B*, 2021, **9**, 694–709.
59 B. Geng, L. Yan, Y. Zhu, W. Shi, H. Wang, J. Mao, L. Ren, J. Zhang, Y. Tian, F. Gao, X. Zhang, J. Chen and J. Zhu, *Adv. Healthcare Mater.*, 2023, **12**, 2202154.
60 H. Zhu, X. Q. Zhang, Q. S. Wang, J. Deng, Z. Z. Zhang, X. X. Zhang, J. Cao and B. He, *J. Mater. Chem. B*, 2022, **10**, 10083–10096.
61 L. Yan, Z. Cao, L. J. Ren, T. T. Zhang, J. Y. Hu, J. K. Chen, X. F. Zhang, B. Liu, C. Q. Feng, J. B. Zhu and B. J. Geng, *Adv. Healthcare Mater.*, 2023, **13**, 232190.
62 Y. Y. Zhang, S. Li, X. Y. Fang, B. P. Miao, Y. J. Wang, J. T. Liu, G. H. Nie and B. Zhang, *Nanophotonics*, 2022, **11**, 5189–5204.

63 X. S. Li, J. F. Lovell, J. Yoon and X. Y. Chen, *Nat. Rev. Clin. Oncol.*, 2020, **17**, 657–674.
64 S. Y. Wu, Y. X. Ye, Q. Zhang, Q. J. Kang, Z. M. Xu, S. Z. Ren, F. Lin, Y. T. Duan, H. J. Xu, Z. Y. Hu, S. S. Yang, H. L. Zhu, M. J. Zou and Z. C. Wang, *Adv. Sci.*, 2023, **10**, 2203742.
65 X. H. Zhu, M. Wang, H. H. Wang, Y. H. Ding, Y. F. Liu, Z. C. Fu, D. Y. Lin, C. H. Lu and X. K. Tu, *Small*, 2022, **18**, 2204951.
66 S. Hameed, P. Bhattarai, Z. R. Gong, X. L. Liang, X. L. Yue and Z. F. Dai, *Nanoscale Adv.*, 2022, **5**, 277–289.
67 S. Wang, C. Zhang, F. Fang, Y. Y. Fan, J. N. Yang and J. F. Zhang, *J. Mater. Chem. B*, 2023, **11**, 8315–8326.
68 H. Bian, D. D. Ma, X. F. Zhang, K. Xin, Y. J. Yang, X. J. Peng and Y. Xiao, *Small*, 2021, **17**, 2100398.
69 S. Zeng, Y. Wang, C. Chen, H. Kim, X. Liu, M. Jiang, Y. Yu, Y. S. Kafuti, Q. Chen, J. Wang, X. Peng, H. Li and J. Yoon, *Angew. Chem., Int. Ed.*, 2024, **63**, 2316487.
70 H. D. Li, J. Y. Wang, H. Kim, X. J. Peng and J. Yoon, *Angew. Chem., Int. Ed.*, 2023, **63**, 2311764.
71 T. Xiong, Y. C. Chen, Q. Peng, S. Lu, S. R. Long, M. L. Li, H. Wang, S. Lu, X. Q. Chen, J. L. Fan, L. Wang and X. J. Peng, *Adv. Mater.*, 2023, **36**, 2309711.
72 Y. C. Chen, J. W. Y. Lam, R. T. K. Kwok, B. Liu and B. Z. Tang, *Mater. Horiz.*, 2019, **6**, 428–433.
73 J. B. Zhuang, B. Wang, H. Chen, K. Y. Zhang, N. Zhao, N. Li and B. Z. Tang, *ACS Nano*, 2023, **17**, 9110–9125.
74 S. L. Song, Y. Zhao, M. M. Kang, F. Zhang, Q. Wu, N. Niu, H. Yang, H. F. Wen, S. Fu, X. Li, Z. J. Zhang, B. Z. Tang and D. Wang, *Adv. Mater.*, 2024, **36**, 2309748.
75 Z. J. Zhang, W. H. Xu, M. M. Kang, H. F. Wen, H. Guo, P. F. Zhang, L. Xi, K. Li, L. Wang, D. Wang and B. Tang, *Adv. Mater.*, 2020, **32**, 2003210.
76 A. L. Antaris, H. Chen, S. Diao, Z. R. Ma, Z. Zhang, S. J. Zhu, J. Wang, A. X. Lozano, Q. L. Fan, L. L. Chew, M. Zhu, K. Cheng, X. C. Hong, H. J. Dai and Z. Cheng, *Nat. Commun.*, 2017, **8**, 15269.
77 Q. L. Yang, Z. B. Hu, S. J. Zhu, R. Ma, H. L. Ma, Z. R. Ma, H. Wan, T. Zhu, Z. Y. Jiang, W. Q. Liu, L. Y. Jiao, H. T. Sun, Y. Y. Liang and H. J. Dai, *J. Am. Chem. Soc.*, 2018, **140**, 1715–1724.
78 Y. Gao, Y. Liu, X. Li, H. Wang, Y. Yang, Y. Luo, Y. Wan, C. S. Lee, S. Li and X. H. Zhang, *Nanoicro Lett.*, 2024, **16**, 21.
79 S. Gao, S. Yu, Y. Zhang, A. Wu, S. Zhang, G. Wei, H. Wang, Z. Xiao and W. Lu, *Adv. Funct. Mater.*, 2021, **31**, 2008356.
80 B. L. Yin, Q. Q. Qin, Z. Li, Y. J. Wang, X. L. Liu, Y. C. Liu, S. Y. Huan, X. B. Zhang and G. S. Song, *Nano Today*, 2022, **45**, 101550.
81 L. Q. Li, C. Shao, T. Liu, Z. C. Chao, H. L. Chen, F. Xiao, H. M. He, Z. X. Wei, Y. L. Zhu, H. Wang, X. D. Zhang, Y. T. Wen, B. Yang, F. He and L. L. Tian, *Adv. Mater.*, 2020, **32**, 2003471.
82 Y. Li, R. B. Tang, X. Y. Liu, J. Y. Gong, Z. J. Zhao, Z. H. Sheng, J. J. Zhang, X. Y. Li, G. L. Niu, R. T. K. Kwok, W. F. Zheng, X. Y. Jiang and B. Z. Tang, *ACS Nano*, 2020, **14**, 16840–16853.
83 G. S. He, L. S. Tan, Q. Zheng and P. N. Prasad, *Chem. Rev.*, 2008, **108**, 1245–1330.
84 M. Pawlicki, H. A. Collins, R. G. Denning and H. L. Anderson, *Angew. Chem., Int. Ed.*, 2009, **48**, 3244–3266.
85 Y. Shen, A. J. Shuhendler, D. Ye, J. J. Xu and H. Y. Chen, *Chem. Soc. Rev.*, 2016, **45**, 6725–6741.
86 L. Jin, S. Shen, Y. Huang, D. Li and X. Yang, *Biomaterials*, 2021, **268**, 120582.
87 X. H. Lin, R. Zhu, Z. Z. Hong, X. Zhang, S. Chen, J. B. Song and H. H. Yang, *Adv. Funct. Mater.*, 2021, **31**, 2101278.
88 K. Wu, H. H. Zhao, Z. Q. Sun, B. Wang, X. Y. Tang, Y. N. Dai, M. X. Li, Q. M. Shen, H. Zhang, Q. L. Fan and W. Huang, *Theranostics*, 2019, **9**, 7697–7713.
89 R. J. Hu, T. M. Guo, C. Y. Zeng, M. M. Chen, X. J. Zhu, L. C. Chen, Y. Q. Dong and F. F. Fu, *New J. Chem.*, 2023, **47**, 628–634.
90 M. Y. Luo, X. Y. Zhu, H. F. Yang, L. Yan, R. Cai, Y. L. Zhao and W. H. Tan, *Nano Today*, 2023, **51**, 101919.
91 M. F. Tsai, S. H. G. Chang, F. Y. Cheng, V. Shanmugam, Y. S. Cheng, C. H. Su and C. S. Yeh, *ACS Nano*, 2013, **7**, 5330–5342.
92 Y. F. Kong, D. Santos-Carballal, D. Martin, N. N. Sergeeva, W. L. Wang, G. S. Liu, B. Johnson, B. Bhayana, Z. A. T. Lin, Y. S. Wang, X. Le Guével, N. H. de Leeuw, D. J. Zhou and M. X. Wu, *Mater. Today*, 2021, **51**, 96–107.
93 J. Beik, M. Khateri, Z. Khosravi, S. K. Kamrava, S. Kooranifar, H. Ghaznavi and A. Shakeri-Zadeh, *Coord. Chem. Rev.*, 2019, **387**, 299–324.
94 Q. Chen, J. W. Chen, Z. J. Yang, L. Zhang, Z. L. Dong and Z. Liu, *Nano Res.*, 2018, **11**, 5657–5669.
95 L. Y. Zhang, C. Liu, Y. Gao, Z. H. Li, J. Xing, W. Z. Ren, L. L. Zhang, A. G. Li, G. M. Lu, A. G. Wu and L. Y. Zeng, *Adv. Healthcare Mater.*, 2018, **7**, 1801144.
96 Z. W. Li, F. Yang, D. Wu, Y. H. Liu, Y. Gao, H. C. Lian, H. X. Zhang, Z. B. Yin, A. G. Wu and L. Y. Zeng, *Nanoscale*, 2020, **12**, 22173–22184.
97 L. Brus, *Nat. Mater.*, 2016, **15**, 824–825.
98 J. Lin, S. J. Wang, P. Huang, Z. Wang, S. H. Chen, G. Niu, W. W. Li, J. He, D. X. Cui, G. M. Lu, X. Y. Chen and Z. H. Nie, *ACS Nano*, 2013, **7**, 5320–5329.
99 J. Wang, X. Zhuo, X. Xiao, R. Mao, Y. Wang, J. Wang and J. Liu, *Nanoscale*, 2019, **11**, 3386–3395.
100 Y. H. Liu, Z. W. Li, Z. B. Yin, H. X. Zhang, Y. Gao, G. Y. Huo, A. G. Wu and L. Y. Zeng, *ACS Appl. Mater. Interfaces*, 2020, **12**, 14866–14875.
101 N. Li, F. Z. Shen, Z. H. Cai, W. Z. Pan, Y. M. Yin, X. Deng, X. Zhang, J. O. Machuki, Y. Y. Yu, D. Z. Yang, Y. Yang, M. Guan and F. L. Gao, *Small*, 2020, **16**, 2005511.
102 X. Li, Z. Hu, J. Ma, X. Wang, Y. Zhang, W. Wang and Z. Yuan, *Colloids Surf., B*, 2018, **167**, 260–266.
103 Y. Feng, Y. Chang, X. Sun, Y. Cheng, R. Zheng, X. Wu, L. Wang, X. Ma, X. Li and H. Zhang, *Biomater. Sci.*, 2019, **7**, 1448–1462.
104 D. Wang, H. Z. Wang, L. Ji, M. Xu, B. Bai, X. D. Wan, D. Y. Hou, Z. Y. Qiao, H. Wang and J. T. Zhang, *ACS Nano*, 2021, **15**, 8694–8705.

105 J. J. Liu, H. N. Liang, M. H. Li, Z. Luo, J. X. Zhang, X. M. Guo and K. Y. Cai, *Biomaterials*, 2018, **157**, 107–124.
106 X. Y. Xu, Y. Chong, X. Y. Liu, H. Fu, C. G. Yu, J. Huang and Z. J. Zhang, *Acta Biomater.*, 2019, **84**, 328–338.
107 C. C. Jian, J. Q. Zhang and X. C. Ma, *RSC Adv.*, 2020, **10**, 13277–13285.
108 L. Zhao, Z. Q. Sun, Y. Wang, J. Huang, H. T. Wang, H. Li, F. Chang and Y. Y. Jiang, *Acta Biomater.*, 2023, **170**, 496–506.
109 A. S. C. Gonçalves, C. F. Rodrigues, A. F. Moreira and I. J. Correia, *Acta Biomater.*, 2020, **116**, 105–137.
110 G. N. Zhang, Z. Z. Wu, Y. Q. Yang, J. Shi, J. Lv, Y. Fang, Z. Shen, Z. Lv, P. C. Li, X. H. Yao, W. Y. Chen, X. C. Wei, P. K. Chu and X. Y. Zhang, *Chem. Eng. J.*, 2022, **428**, 131155.
111 H. Du, F. Yang, C. Y. Yao, W. H. Lv, H. Peng, S. G. Stanciu, H. A. Stenmark, Y. M. Song, B. Jiang and A. G. Wu, *Biomaterials*, 2022, **291**, 121868.
112 H. Du, F. Yang, C. Y. Yao, Z. C. Zhong, P. H. Jiang, S. G. Stanciu, H. Peng, J. P. Hu, B. Jiang, Z. H. Li, W. H. Lv, F. Zheng, H. A. Stenmark and A. G. Wu, *Small*, 2022, **18**, 2201669.
113 H. Du, O. U. Akakuru, C. Yao, F. Yang and A. Wu, *Transl. Oncol.*, 2022, **15**, 101264.
114 C. Y. Yao, F. Yang, L. Sun, Y. Y. Ma, S. G. Stanciu, Z. H. Li, C. Liu, O. U. Akakuru, L. P. Xu, N. Hampp, H. M. Lu and A. G. Wu, *Nano Today*, 2020, **35**, 100967.
115 Y. W. Wang, Y. M. Li, Z. J. Zhang, L. Wang, D. Wang and B. Z. Tang, *Adv. Mater.*, 2021, **33**, 2103748.
116 Y. B. Pan, Y. Zhu, C. X. Xu, C. S. Pan, Y. Shi, J. H. Zou, Y. Y. Li, X. Y. Hu, B. Zhou, C. Y. Zhao, Q. Q. Gao, J. M. Zhang, A. G. Wu, X. Y. Chen and J. Li, *ACS Nano*, 2022, **16**, 19038–19052.
117 J. Yao, F. Zheng, F. Yang, C. Yao, J. Xing, Z. Li, S. Sun, J. Chen, X. Xu, Y. Cao, N. Hampp and A. Wu, *Biomater. Sci.*, 2021, **9**, 7591–7602.
118 M. Chang, Z. Hou, D. Jin, J. Zhou, M. Wang, M. Wang, M. Shu, B. Ding, C. Li and J. Lin, *Adv. Mater.*, 2020, **32**, 2004647.
119 R. Sun, W. Ma, M. J. Ling, C. H. Tang, M. Zhong, J. Y. Dai, M. Y. Zhu, X. Z. Cai, G. Li, Q. Xu, L. G. Tang, Z. Q. Yu and Z. W. Peng, *J. Controlled Release*, 2022, **350**, 525–537.
120 S. Lany, *J. Phys. Condens. Mater.*, 2015, **27**, 283203.
121 E. Pastor, M. Sachs, S. Selim, J. R. Durrant, A. A. Bakulin and A. Walsh, *Nat. Rev. Mater.*, 2022, **7**, 503–521.
122 D. F. Yan, Y. X. Li, J. Huo, R. Chen, L. M. Dai and S. Y. Wang, *Adv. Mater.*, 2017, **29**, 1606459.
123 M. T. Liu, J. Ye, S. Liu, X. P. Xu, Y. J. Cui, J. W. Qu, Z. Y. Zhang, K. F. Zhang, N. Niu, L. G. Chen, Y. J. Fu and J. T. Xu, *Adv. Funct. Mater.*, 2023, **33**, 2306392.
124 N. Li, H. Gao, X. Wang, S. J. Zhao, D. Lv, G. Q. Yang, X. Y. Gao, H. K. Fan, Y. Q. Gao and L. Ge, *Chin. J. Catal.*, 2020, **41**, 426–434.
125 S. Shin, J. Lee, J. Han, F. Li, D. Ling and W. Park, *Tissue Eng. Regen. Med.*, 2022, **19**, 205–219.
126 Y. Chao and Z. Liu, *Nat. Rev. Bioeng.*, 2023, **1**, 125–138.
127 Y. N. Luo, L. L. Zhang, S. L. Wang, Y. Wang, J. Hua, C. C. Wen, S. L. Zhao and H. Liang, *ACS Appl. Mater. Interfaces*, 2023, **15**, 38309–38322.
128 Q. Wang, B. T. Qu, J. Li, Y. Q. Liu, J. Dong, X. Y. Peng and R. P. Zhang, *ACS Appl. Mater. Interfaces*, 2022, **14**, 4980–4994.
129 T. Bao, W. Y. Yin, X. P. Zheng, X. Zhang, J. Yu, X. H. Dong, Y. Yong, F. P. Gao, L. Yan, Z. J. Gu and Y. L. Zhao, *Biomaterials*, 2016, **76**, 11–24.
130 W. Y. Yin, T. Bao, X. Zhang, Q. Gao, J. Yu, X. H. Dong, L. Yan, Z. J. Gu and Y. L. Zhao, *Nanoscale*, 2018, **10**, 1517–1531.
131 Q. Liu, B. Wu, M. Y. Li, Y. Y. Huang and L. L. Li, *Adv. Sci.*, 2022, **9**, 2103911.
132 O. Inganäs, *Adv. Mater.*, 2018, **30**, 1802808.
133 H. Peng, S. X. Li, J. Xing, F. Yang and A. G. Wu, *J. Mater. Chem. B*, 2023, **11**, 5238–5250.
134 J. F. Wang, S. G. Ping, M. Lin, L. B. Fu, Y. S. Liu, L. L. Han, S. D. Chen, X. Wang, M. Y. Lu, Z. Q. Luo, Y. Zhong, B. Y. Shi and F. Bai, *ACS Nano*, 2023, **17**, 16840–16853.
135 Z. Gu, Z. Guo, S. Gao, L. Huang and Z. Liu, *ACS Nano*, 2023, **17**, 10152–10163.
136 Y. L. Liu, Y. Liang, P. P. Lei, Z. Zhang and Y. M. Chen, *Adv. Sci.*, 2023, **10**, 2203669.
137 W. L. Li, H. Xin, Y. N. Zhang, C. Feng, Q. D. Li, D. X. Kong, Z. F. Sun, Z. W. Xu, J. M. Xiao, G. Tian, G. L. Zhang and L. Liu, *Small*, 2022, **18**, 2205647.
138 C. S. Li, J. Ye, X. Yang, S. Liu, Z. Y. Zhang, J. Wang, K. F. Zhang, J. T. Xu, Y. J. Fu and P. P. Yang, *ACS Nano*, 2022, **16**, 18143–18156.
139 S. Yan, X. Zeng, Y. Tang, B. F. Liu, Y. Wang and X. Liu, *Adv. Mater.*, 2019, **31**, 1905825.
140 Q. Sun, W. Chen, M. Wang, P. Zheng, M. Gao, F. Song and C. Li, *Adv. Healthcare Mater.*, 2023, **12**, 2301087.
141 X. B. Zhang, W. W. Chen, X. Y. Xie, Y. Y. Li, D. S. Chen, Z. C. Chao, C. H. Liu, H. B. Ma, Y. Liu and H. X. Ju, *Angew. Chem., Int. Ed.*, 2019, **58**, 12117–12122.
142 Q. Ci, Y. Wang, B. Wu, E. Coy, J. J. Li, D. Jiang, P. Zhang and G. Wang, *Adv. Sci.*, 2023, **10**, 2206271.
143 T. Han, Y. Wang, S. Ma, M. Li, N. Zhu, S. Tao, J. Xu, B. Sun, Y. Jia, Y. Zhang, S. Zhu and B. Yang, *Adv. Sci.*, 2022, **9**, 2203474.
144 H. Lin, S. Gao, C. Dai, Y. Chen and J. Shi, *J. Am. Chem. Soc.*, 2017, **139**, 16235–16247.
145 X. G. Zhang, X. M. Chen, P. Zhang, M. T. Li, M. Feng, Y. Q. Zhang, L. L. Cheng, J. J. Tang, L. T. Xu, Y. D. Liu, Z. Y. Liu, Z. Cao and J. Liu, *Nano Res.*, 2022, **16**, 7148–7163.
146 Z. Tian, X. T. Zhang, D. Li, D. Zhou, P. T. Jing, D. Z. Shen, S. N. Qu, R. Zboril and A. L. Rogach, *Adv. Opt. Mater.*, 2017, **5**, 1700416.
147 D. Li, P. T. Jing, L. H. Sun, Y. An, X. Y. Shan, X. H. Lu, D. Zhou, D. Han, D. Z. Shen, Y. C. Zhai, S. N. Qu, R. Zboril and A. L. Rogach, *Adv. Mater.*, 2018, **30**, 1705913.
148 D. Li, C. Liang, E. V. Ushakova, M. H. Sun, X. D. Huang, X. Y. Zhang, P. T. Jing, S. J. Yoo, J. G. Kim, E. S. Liu,

W. Zhang, L. H. Jing, G. C. Xing, W. T. Zheng, Z. K. Tang, S. N. Qu and A. L. Rogach, *Small*, 2019, **15**, 1905050.
149 A. Sundaram, J. S. Ponraj, C. Wang, W. K. Peng, R. K. Manavalan, S. C. Dhanabalan, H. Zhang and J. Gaspar, *J. Mater. Chem. B*, 2020, **8**, 4990–5013.
150 Z. Hao, Y. Li, X. Liu, T. Jiang, Y. He, X. Zhang, C. Cong, D. Wang, Z. Liu and D. Gao, *Chem. Eng. J.*, 2021, **425**, 130639.
151 S. Y. Hao, H. C. Han, Z. Y. Yang, M. T. Chen, Y. Y. Jiang, G. X. Lu, L. Dong, H. L. Wen, H. Li, J. R. Liu, L. L. Wu, Z. Wang and F. L. Wang, *Nano-Micro Lett.*, 2022, **14**, 178.
152 X. Y. Zhu, W. Q. Zhang, H. D. Xiang, Q. C. Chang, R. X. Liu, Y. L. Wan, R. T. Zhang, F. Zhao, Y. X. She, H. Yuan, J. G. Yang, Q. Q. Li, S. S. Wang and L. Yan, *Nano Today*, 2023, **50**, 101836.
153 F. H. Duan, Q. J. Jia, G. L. Liang, M. F. Wang, L. Zhu, K. J. McHugh, L. H. Jing, M. Du and Z. H. Zhang, *ACS Nano*, 2023, **17**, 11290–11308.
154 Y. Rao, G. Xu, Z. Zhang, W. Wang, C. Zhang, M. Zhao, Y. Qu, W. Li, M. Ji, Y. Liu and Y. Q. Li, *Chem. Eng. J.*, 2023, **465**, 142961.
155 Z. Li, Z. Zhou, Y. Wang, J. Wang, L. Zhou, H. B. Cheng and J. Yoon, *Coord. Chem. Rev.*, 2023, **493**, 215324.
156 L. M. Wang, K. K. Kang, H. Y. Hou, Y. J. Ma, K. Yu, F. Y. Qu and H. M. Lin, *J. Colloid Interface Sci.*, 2022, **625**, 145–157.
157 J. L. Li, H. L. Peng, C. C. Wen, P. J. Xu, X. C. Shen and C. J. Gao, *Langmuir*, 2022, **38**, 5502–5514.
158 S. L. Zeng, J. Q. Chen, R. K. Gao, R. Chen, Q. Xue, Y. G. Ren, L. J. Liu, C. Y. Tang, H. Y. Hu, N. Zeng, S. Wen, H. Zhang, C. B. Liu and C. H. Fang, *Adv. Mater.*, 2023, **36**, 2308780.
159 X. Y. Wang, C. W. Li, J. C. Qian, X. T. Lv, H. Li, J. L. Zou, J. H. Zhang, X. F. Meng, H. J. Liu, Y. Qian, W. C. Lin and H. Wang, *Small*, 2021, **17**, 11290–11308.
160 H. S. Zhao, Z. W. Liu, Y. Wei, L. Zhang, Z. Wang, J. S. Ren and X. G. Qu, *ACS Nano*, 2022, **16**, 20353–20363.
161 B.-Q. Chen, Y. Zhao, Y.-J. Pan, D.-G. Zhang, H. Liu, Y.-H. Shi, C.-Y. Li, R. K. Kankala, Y. Zhang, S.-B. Wang, G. Liu and A.-Z. Chen, *ACS Mater. Lett.*, 2023, **6**, 321–334.
162 B. Yang, Y. Zhang, L. Sun, J. Wang, Z. Zhao, Z. Huang, W. Mao, R. Xue, R. Chen, J. Luo, T. Wang, J. Jiang and Y. Qin, *Adv. Funct. Mater.*, 2022, **33**, 2211251.
163 Y. Zhang, Q. Wang, Y. S. Ji, L. Y. Fan, B. B. Ding, J. Lin and L. L. Wang, *Chem. Eng. J.*, 2022, **435**, 134869.
164 L. J. Jin, S. Shen, Y. J. Huang, D. D. Li and X. Z. Yang, *Biomaterials*, 2021, **268**, 120582.
165 L. An, C. Wang, Q. Tian, C. Tao, F. Xue, S. Yang, X. Zhou, X. Chen and G. Huang, *Nano Today*, 2022, **43**, 101397.
166 M. Chang, M. Wang, M. Wang, M. Shu, B. Ding, C. Li, M. Pang, S. Cui, Z. Hou and J. Lin, *Adv. Mater.*, 2019, **31**, 1905271.
167 K. K. Kang, L. M. Wang, Y. J. Ma, K. Yu, J. W. Liu, F. Y. Qu and H. M. Lin, *Carbon*, 2022, **197**, 98–111.
168 C. Yang, M. R. Younis, J. Zhang, J. L. Qu, J. Lin and P. Huang, *Small*, 2020, **16**, 2001518.
169 L. M. Wang, K. K. Kang, Y. J. Ma, F. Zhang, W. Guo, K. Yu, K. Wang, F. Y. Qu and H. M. Lin, *Chem. Eng. J.*, 2022, **444**, 136512.
170 Q. Q. Sun, F. He, H. T. Bi, Z. Wang, C. Q. Sun, C. X. Li, J. T. Xu, D. Yang, X. X. Wang, S. L. Gai and P. P. Yang, *Chem. Eng. J.*, 2019, **362**, 679–691.
171 W. W. Zeng, H. J. Zhang, Y. M. Deng, A. T. Jiang, X. Y. Bao, M. Q. Guo, Z. M. Li, M. Y. Wu, X. Y. Ji, X. W. Zeng and L. Mei, *Chem. Eng. J.*, 2020, **389**, 124494.
172 B. Chen, T. Roskams and P. A. M. de Witte, *Lasers Surg. Med.*, 2002, **31**, 158–163.
173 M. Overchuk, R. A. Weersink, B. C. Wilson and G. Zheng, *ACS Nano*, 2023, **17**, 7979–8003.
174 T. Christensen, A. Wahl and L. Smedshammer, *Br. J. Cancer*, 1984, **50**, 85–89.
175 Q. Q. Sun, Z. Wang, B. Liu, T. Jia, C. Wang, D. Yang, F. He, S. L. Gai and P. P. Yang, *Chem. Eng. J.*, 2020, **390**, 124624.
176 Y. Su, K. Lu, Y. Huang, J. Zhang, X. Sun, J. Peng, Y. Zhou and L. Zhao, *Biomaterials*, 2023, **294**, 122017.
177 M. Hiraoka and G. M. Hahn, *Cancer Res.*, 1989, **49**, 3734–3736.
178 Z. M. Tang, P. R. Zhao, D. L. Ni, Y. Y. Liu, M. Zhang, H. Wang, H. Zhang, H. B. Gao, Z. W. Yao and W. B. Bu, *Mater. Horiz.*, 2018, **5**, 946–952.
179 B. Chen, Y. Xu, P. Agostinis and P. A. M. De Witte, *Int. J. Oncol.*, 2001, **18**, 1279–1285.
180 S. Zhang, L. N. Wu, W. Q. Shi, J. C. Qin, W. Feng, Y. Chen and R. F. Zhang, *Adv. Funct. Mater.*, 2023, **33**, 2302360.
181 Y. C. Wang, X. Y. Dai, C. H. Dong, W. T. Guo, Z. W. Xu, Y. Chen, H. J. Xiang and R. F. Zhang, *Adv. Mater.*, 2022, **34**, 2106773.
182 Y. C. Wang, X. Y. Dai, L. A. Wu, H. J. Xiang, Y. Chen and R. F. Zhang, *Biomaterials*, 2023, **299**, 122178.
183 R. Beck, N. Dejeans, C. Glorieux, M. Creton, E. Delaive, M. Dieu, M. Raes, P. Levêque, B. Gallez, M. Depuydt, J. F. Collet, P. B. Calderon and J. Verrax, *PLoS One*, 2012, **7**, 40795.
184 L. Chen, G. J. Chen, K. Hu, L. X. Chen, Z. Y. Zeng, B. Li, G. H. Jiang and Y. Liu, *Chem. Eng. J.*, 2023, **468**, 143685.
185 G. D. Gong, J. Z. Pan, Y. X. He, J. J. Shang, X. L. Wang, Y. Y. Zhang, G. L. Zhang, F. Wang, G. Zhao and J. L. Guo, *Theranostics*, 2022, **12**, 2028–2040.
186 S. Kuang, F. M. Wei, J. Karges, L. B. Ke, K. Xiong, X. X. Liao, G. Gasser, L. N. Ji and H. Chao, *J. Am. Chem. Soc.*, 2022, **144**, 4091–4101.
187 Z. H. Su, D. M. Xi, Y. C. Chen, R. Wang, X. L. Zeng, T. Xiong, X. Xia, X. Rong, T. Liu, W. K. Liu, J. J. Du, J. L. Fan, X. J. Peng and W. Sun, *Small*, 2023, **19**, 2205825.
188 J. Yuan, Q. H. Zhou, S. Xu, Q. P. Zuo, W. Li, X. X. Zhang, T. B. Ren, L. Yuan and X. B. Zhang, *Angew. Chem., Int. Ed.*, 2022, **61**, 2206169.
189 F. A. Deng, Y. B. Liu, R. R. Zheng, R. J. Kong, X. Zhou, J. J. Wang, H. Cheng and S. Y. Li, *ACS Appl. Nano Mater.*, 2022, **5**, 9277–9285.
190 H. Z. He, L. H. Du, H. M. Xue, J. Wu and X. T. Shuai, *Acta Biomater.*, 2022, **149**, 297–306.

191 M. Warszy, P. Repetowski and J. M. Dabrowski, *Coord. Chem. Rev.*, 2023, **495**, 215350.
192 J. Choi, I. C. Sun, H. S. Hwang, H. Y. Yoon and K. Kim, *Adv. Drug Delivery Rev.*, 2022, **186**, 114344.
193 M. Y. Wang, M. Y. He, M. Y. Zhang, S. J. Xue, T. Xu, Y. N. Zhao, D. Z. Li, F. Zhi and D. W. Ding, *Biomaterials*, 2023, **301**, 122257.
194 N. N. Wang, Y. X. Zhou, Y. W. Xu, X. M. Ren, S. Y. Zhou, Q. Shang, Y. Jiang and Y. X. Luan, *Chem. Eng. J.*, 2020, **400**, 125995.
195 Y. Zhou, S. N. Liu, C. L. Hu, L. H. Cai and M. L. Pang, *J. Mater. Chem. B*, 2020, **8**, 5451–5459.
196 Y. Y. Guo, Q. S. Zhang, Q. W. Zhu, J. Gao, X. Y. Zhu, H. J. Yu, Y. H. Li and C. Zhang, *Sci. Adv.*, 2022, **8**, eabn2941.
197 P. Zhang, Y. Cui and Y. Wang, *Nano Today*, 2023, **49**, 101816.
198 G. Canti, D. Lattuada, A. Nicolin, P. Taroni, G. Valentini and R. Cubeddu, *Anti-Cancer Drugs*, 1994, **5**, 443–447.
199 L. Q. Gao, C. R. Zhang, D. Gao, H. Liu, X. H. Yu, J. H. Lai, F. Wang, J. Lin and Z. F. Liu, *Theranostics*, 2016, **6**, 627–637.
200 G. X. Lan, K. Y. Ni, Z. W. Xu, S. S. Veroneau, Y. Song and W. B. Lin, *J. Am. Chem. Soc.*, 2018, **140**, 5670–5673.
201 P. Zhang, Y. Y. Cui and Y. L. Wang, *Nano Today*, 2023, **49**, 101816.
202 X. L. Li, C. Jiang, Q. H. Wang, S. B. Yang, Y. Y. Cao, J. N. Hao, D. C. Niu, Y. Chen, B. Han, X. Jia, P. Zhang and Y. S. Li, *Adv. Sci.*, 2022, **9**, 2104671.
203 J. Y. Z. Wu, Y. F. Zhang, K. J. Jiang, X. Y. Wang, N. T. Blum, J. Zhang, S. S. Jiang, J. Lin and P. Huang, *Adv. Mater.*, 2022, **34**, 2200062.
204 Z. H. Zhou, J. S. Huang, Z. Y. Zhang, L. Zhang, Y. Cao, Z. G. Xu, Y. J. Kang and P. Xue, *Chem. Eng. J.*, 2022, **435**, 135085.
205 Z. J. Lv, L. H. Jin, W. H. Gao, Y. Cao, H. Zhang, D. Z. Xue, N. Yin, T. Q. Zhang, Y. H. Wang and H. J. Zhang, *ACS Appl. Mater. Interfaces*, 2022, **14**, 30523–30532.
206 X. Gao, J. Feng, S. Y. Song, K. Liu, K. M. Du, Y. F. Zhou, K. H. Lv and H. J. Zhang, *Nano Today*, 2022, **43**, 101433.
207 H. J. Hao, M. M. Sun, P. Y. Li, J. W. Sun, X. Y. Liu and W. P. Gao, *ACS Appl. Mater. Interfaces*, 2019, **11**, 9756–9762.
208 H. W. Zhang, F. Lu, W. Pan, Y. G. Ge, B. J. Cui, S. H. Gong, N. Li and B. Tang, *Biomater. Sci.*, 2021, **9**, 3814–3820.
209 Z. Z. Yu, P. Zhou, W. Pan, N. Li and B. Tang, *Nat. Commun.*, 2018, **9**, 5044.
210 K. Lv, L. Wang, Y. Ma, F. Zhang, W. Guo, K. Yu, F. Qu and H. Lin, *Biomater. Adv.*, 2022, **136**, 212778.
211 C. Y. Cao, N. Yang, X. R. Wang, J. J. Shao, X. J. Song, C. Liang, W. J. Wang and X. C. Dong, *Coord. Chem. Rev.*, 2023, **491**, 215245.
212 C. Szabo, *Nat. Rev. Drug Discovery*, 2016, **15**, 185–203.
213 Y. S. Wang, T. Yang and Q. J. He, *Nat. Sci. Rev.*, 2020, **7**, 1485–1512.
214 K. Y. Wang, Y. Li, X. Wang, Z. J. Zhang, L. P. Cao, X. Y. Fan, B. Wan, F. X. Liu, X. B. Zhang, Z. G. He, Y. T. Zhou, D. Wang, J. Sun and X. Y. Chen, *Nat. Commun.*, 2023, **14**, 2950.
215 P. Ji, K. X. Yang, Q. Q. Xu, G. L. Qin, Q. Y. Zhu, Y. Qian and W. S. Yao, *Pharmaceuticals*, 2023, **16**, 1394.
216 J. Jiang, J. Xie, L. Zhou, W. Han, J. Ye, D. Hu, W. Xie, J. Qiu, R. Chen and X. Wang, *Chem. Eng. J.*, 2024, **480**, 147850.
217 G. H. Luo, Z. H. Li, M. L. Chen, J. Z. Zheng, X. N. A. Deng, G. Xu, M. Cheng, X. M. Li and Y. H. Duo, *Chem. Eng. J.*, 2022, **442**, 136169.
218 F. R. Liu, S. L. Gong, M. L. Shen, T. He, X. Q. Liang, Y. Q. Shu, X. X. Wang, S. Ma, X. C. Li, M. M. Zhang, Q. J. Wu and C. Y. Gong, *Chem. Eng. J.*, 2021, **403**, 126305.
219 W. Y. Yu, T. Liu, M. K. Zhang, Z. X. Wang, J. J. Ye, C. X. Li, W. L. Liu, R. Q. Li, J. Feng and X. Z. Zhang, *ACS Nano*, 2019, **13**, 1784–1794.
220 W. H. Jin, Y. J. Wu, W. Z. Li, J. Wang, K. Yang, P. Song, L. B. Zhu, W. W. Zhang, L. Gui and F. Ge, *ACS Appl. Nano Mater.*, 2023, **6**, 18880–18891.
221 Z. Yuan, C. C. Lin, Y. He, B. L. Tao, M. W. Chen, J. X. Zhang, P. Liu and K. Y. Cai, *ACS Nano*, 2020, **14**, 3546–3562.
222 H. A. Tian, Y. Li, J. Y. Lin, F. K. Zhu, Z. Q. Hou, P. Y. Wang and X. L. Liu, *ACS Mater. Lett.*, 2023, **5**, 2542–2555.
223 M. Y. Chang, M. Wang, Y. H. Liu, M. Liu, A. A. Al Kheraif, P. A. Ma, Y. L. Zhao and J. Lin, *Small*, 2022, **19**, 2206423.
224 L. Wu, Y. Liu, W. Zeng, Y. Ishigaki, S. Zhou, X. Wang, Y. Sun, Y. Zhang, X. Jiang, T. Suzuki and D. Ye, *J. Am. Chem. Soc.*, 2023, **145**, 27838–27849.
225 V. N. Astratov, Y. B. Sahel, Y. C. Eldar, L. Huang, A. Ozcan, N. heludev, J. Zhao, Z. Burns, Z. Liu, E. Narimanov, N. Goswami, G. Popescu, E. Pfitzner, P. Kukura, Y. T. Hsiao, C. L. Hsieh, B. Abbey, A. Diaspro, A. LeGratiet, P. Bianchini, N. T. Shaked, B. Simon, N. Verrier, M. Debailleul, O. Haeberlé, S. Wang, M. Liu, Y. Bai, J. X. Cheng, B. S. Kariman, K. Fujita, M. Sinvani, Z. Zalevsky, X. Li, G. J. Huang, S. W. Chu, O. Tzang, D. Hershkovitz, O. Cheshnovsky, M. J. Huttunen, S. G. Stanciu, V. N. Smolyaninova, I. I. Smolyaninov, U. Leonhardt, S. Sahebdivan, Z. Wang, B. Luk'yanchuk, L. Wu, A. V. Maslov, B. Jin, C. R. Simovski, S. Perrin, P. Montgomery and S. Lecler, *Laser Photon. Rev.*, 2023, **17**, 2200029.
226 S. G. Stanciu, K. König, Y. M. Song, L. Wolf, C. A. Charitidis, P. Bianchini and M. Goetz, *Biophys. Rev.*, 2023, **4**, 021307.
227 G. Tortarolo, A. Zunino, S. Piazza, M. Donato, S. Zappone, A. Pierzyńska-Mach, M. Castello and G. Vicidomini, *Adv. Photonics*, 2024, **6**, 016003.
228 S. G. Stanciu, R. Hristu, G. A. Stanciu, D. E. Tranca, L. Eftimie, A. Dumitru, M. Costache, H. A. Stenmark, H. Manders, A. Cherian, M. Tark-Dame and E. M. M. Manders, *Proc. Natl. Acad. Sci. U. S. A.*, 2022, **119**, e2214662119.
229 C. J. Gao, W. W. Guo, X. L. Guo, Z. Y. Ding, Y. W. Ding and X. C. Shen, *Acta Biomater.*, 2021, **129**, 220–234.

230 Y. He, Y. Pan, X. Zhao, W. Fan, Y. Cai and X. Mou, *Acta Biomater.*, 2022, **152**, 546–561.
231 Z. Liu, Z. Feng, M. Chen, J. Zhan, R. Wu, Y. Shi, Y. Xue, R. Liu, J. J. Zhu and J. Zhang, *Chem. Sci.*, 2023, **14**, 4102–4113.
232 X. Chai, D. Yi, C. Sheng, J. Zhao and L. Li, *Angew. Chem., Int. Ed.*, 2023, **62**, 2217702.
233 Q. Li, H. Fan, Y. Xu, M. Liu, J. Liu, L. Xu, M. Zou, Q. Cheng, Y. Zhang, T. Liang, L. Shi, X. Hu, L. Wang and Z. Wang, *Chem. Eng. J.*, 2023, **458**, 141314.
234 G. Wan, X. Chen, J. Chen, R. Gou, H. Wang, S. Liu, M. Zhang, H. Chen, D. Wang and Q. Zhang, *Biomater. Sci.*, 2023, **11**, 1876–1894.

